Doppler Broadening Addition to Geant4 Code

Introduction

This report is the summary of the testing performed on the Doppler Broadening extension written for Geant4 simulation package by Dr. Marc Kippen of Los Alamos National Laboratory (http://nis-www.lanl.gov/~mkippen/actsim/g4lecs/). The testing was performed using versions Geant4_4.1p01 and Geant4_5.2p01 of GEometry ANd Tracking software and G4LECS_1.01 and G4LECS_1.03 versions of Low-Energy Compton Scattering Package.

A concise summary of what LECS package is all about is given at http://nis-www.lanl.gov/~mkippen/actsim/g4lecs/ :

G4LECS is an extension program for the GEANT4 simulation package that incorporates detailed physics into the simulation of Compton and Rayleigh scattering. In standard GEANT4, the free electron approximation is used for Compton scattering, and Rayleigh scattering is ignored. The G4LowEnergy extension package included in the GEANT4 distribution corrects the Compton cross sections and for bound electron momentum, but does not account for the resulting changes in the scattered particle energies (known as Doppler broadening). Furthermore, there are errors in the treatment of Rayleigh scattering.

These problems lead to significant errors in simulating photon scattering at energies near/below several hundred keV. The G4LECS treatment of Compton scattering accounts for bound electron momentum on a shell-by-shell basis using evaluated data read from tables. For Rayleigh scattering, G4LECS uses evaluated coherent scattering cross section and form factor data read from tables.

G4LECS was designed to be used transparently with any GEANT4 application. It is particularly useful for simulating advanced Compton telescopes, where the fine position and energy resolution make the inclusion of Doppler broadening crucial for realistic simulations.

To our best knowledge, no convenient experimental data exist to serve as a base for the direct comparison with the simulated Doppler broadening effect. Thus, our testing was limited to the code verification and very extensive running of the code in various setups. Also, Carolyn Lehner from the Department of Nuclear and Radiological Sciences at the University of Michigan performed comparison of our simulation results to some semi-analytical results.

The Low Energy Compton Scattering with Doppler broadening—the essential part of the LECS package was tested very extensively, and the results are presented in this report. The part of LECS package dealing with Rayleigh scattering was not specifically tested, but no odd behavior was noticed with respect to that physical process as implemented in LECS. The full LECS package (both Compton and Rayleigh parts) is heavily used in modeling by our group at NRL.

Uncertainty in Energy of the Scattered Gamma-Ray as a Result of Doppler Broadening

When Compton scattering is modeled by the exact Compton formula, as it is done in the regular Geant4 package (without LECS), a specified energy of the incoming gamma-ray and a specified scattering angle mean one and only one energy of the scattered gamma-ray. Taking into account Doppler broadening means allowing the energy of the scattered gamma-ray to obey a certain distribution. In our first set of tests, we tried to reproduce this distribution for several incoming energies, several scattering angles and several materials. Not all of the materials are relevant for the detector physics though, since we tried to cover a wide range of atomic numbers.

Simulation Setup

The relevant part of the physics list used in the simulation is shown below.

```
// -----------------------------------------------------------------------
// Construct and register all EM processes (low energy physics).

void PhysicsList::
ConstructEM()
{
    theParticleIterator->reset();

    while( (*theParticleIterator)() )
    {

        G4ParticleDefinition* particle = theParticleIterator->value();
        G4ProcessManager* pManager = particle->GetProcessManager();
        G4String particleName = particle->GetParticleName();

        if (particleName == "gamma")
        {
            G4LowEnergyPhotoElectric*   theLEPhotoElectric   = new G4LowEnergyPhotoElectric();
            G4LowEnergyGammaConversion* theLEGammaConversion = new G4LowEnergyGammaConversion();

            // Doppler ON
            G4LECSCompton*              theLECompton         = new G4LECSCompton();
            G4LECSRayleigh*             theLERayleigh        = new G4LECSRayleigh();

            // Doppler OFF
```

```
//          G4LowEnergyCompton*          theLECompton          = new G4LowEnergyCompton();
//          G4LowEnergyRayleigh*         theLERayleigh         = new G4LowEnergyRayleigh();

        pManager->AddDiscreteProcess(theLEPhotoElectric);
        pManager->AddDiscreteProcess(theLECompton);
        pManager->AddDiscreteProcess(theLERayleigh);
        pManager->AddDiscreteProcess(theLEGammaConversion);
    }
    else if (particleName == "e-")
    {
        G4LowEnergyIonisation*      theLEIonisation               = new G4LowEnergyIonisation();
        G4LowEnergyBremsstrahlung* theLEBremsstrahlung            = new G4LowEnergyBremsstrahlung();
        G4MultipleScattering*       theEMinusMultipleScattering = new G4MultipleScattering();

        pManager->AddProcess(theEMinusMultipleScattering,-1, 1,1);
        pManager->AddProcess(theLEIonisation,             -1, 2,2);
        pManager->AddProcess(theLEBremsstrahlung,         -1,-1,3);
    }
    else if (particleName == "e+")
    {
        G4MultipleScattering* theEPlusMultipleScattering = new G4MultipleScattering();
        G4eIonisation*        theEPlusIonisation          = new G4eIonisation();
        G4eBremsstrahlung*    theEPlusBremsstrahlung      = new G4eBremsstrahlung();
        G4eplusAnnihilation*  theEPlusAnnihilation        = new G4eplusAnnihilation();

        pManager->AddProcess(theEPlusMultipleScattering,-1, 1,1);
        pManager->AddProcess(theEPlusIonisation,          -1, 2,2);
        pManager->AddProcess(theEPlusBremsstrahlung,      -1,-1,3);
        pManager->AddProcess(theEPlusAnnihilation,         0,-1,4);
    }
  }
}
```

Switching between regular Geant4 and LECS extension was achieved by commenting out the appropriate lines above and recompiling the program.

The following energies of the incoming gamma-ray were chosen for the simulation: 100 keV, 200 keV, 400 keV, 800 keV, 1.6 MeV, and 3.2 MeV. The following scattering angles were considered: 30 degrees, 60 degrees, 90 degrees, and 120 degrees. Compton scattering for the following materials was modeled: Carbon, Silicon, Germanium, Cadmium, and Lead.

We wanted to obtained an energy distribution for the scattered gamma-ray for each of the incoming energies, each of the scattering angles and each material. The following strategy was employed. The photons were shot directly into a large (several meters in each direction) block of material. A check was setup in the user supplied Stepping Action to catch the very first Compton interaction of the incoming gamma (so that the energy of the incoming gamma is exactly the energy being tested). When the required Compton interaction was identified, another check was performed, this time with the intention to select the scattering angles we were testing for. To accomplish this, the observed scattering angle of the current interaction was computed and then compared to the list of angles of interest (kept in `runManager->m_collectionAnglePerRun`). If the difference between the observed scattering angle and one of the angles in the array `runManager->m_collectionAnglePerRun` was less than the specified tolerance, the energy of the scattered (outgoing) gamma was recorded and later on tabulated (in the user supplied `EventAction::EndOfEventAction()`). The value of the crucial tolerance constant (`runManager->m_angleDeltaPerRun`) was chosen to be 0.01 degree (we will discuss the reason for choosing such a small value later).

The relevant portions of the code for the `main()` function and the user supplied Stepping Action are shown below.

```
    for (int energyCounter = 0; energyCounter < 6; ++energyCounter)
    {
        runManager->m_energyOfPrimaryGammaPerRun = 100.* keV * pow(2.0, energyCounter);

        for (int angleCounter = 0; angleCounter < N_ANGLES; ++angleCounter)
        {
```

```
            int angleInt = 30 + 30 * angleCounter;
            runManager->m_collectionAnglePerRun[angleCounter] = double(angleInt) * deg;
        }

        runManager->m_angleDeltaPerRun = double(0.01)*deg;
        runManager->BeamOn(500000000);
    }
```

```
// -------------------------------------------------------------------------
// Virtual method of the base class G4UserSteppingAction.
// This method is invoked at the end of each step.

void
SteppingAction::
UserSteppingAction(
    G4Step const* pStepData)
{
    // Get run manager pointer. Run manager keeps gun setup information and all statistical results
    RunManager* runManager = static_cast<RunManager*>(G4RunManager::GetRunManager());

    G4Track const* pTrack = pStepData->GetTrack();

    // If this is the primary gamma, check it out
    if( (G4Gamma::Gamma()== pTrack->GetDefinition()) && (pTrack->GetParentID() == 0) &&
        (pStepData->GetPreStepPoint()->GetKineticEnergy() == runManager->m_energyOfPrimaryGammaPerRun) )
    {
        G4String processName = ' ';
        G4VProcess const* processStep = pStepData->GetPostStepPoint()->GetProcessDefinedStep();
        if(processStep)
        {
            processName = processStep->GetProcessName();

            if ( (processName == "LowEnCompton") || (processName == "G4LECSComp1.01") )
            {
                G4ThreeVector const& before = pStepData->GetPreStepPoint()->GetMomentumDirection();
                G4ThreeVector const& after = pStepData->GetPostStepPoint()->GetMomentumDirection();
                G4double angle = after.angle(before);

                for (int angleCounter = 0; angleCounter < N_ANGLES; ++angleCounter)
                {
                    G4double trialAngle = runManager->m_collectionAnglePerRun[angleCounter];

                    if ( (angle >= (trialAngle - runManager->m_angleDeltaPerRun)) &&
                         (angle <= (trialAngle + runManager->m_angleDeltaPerRun)) )
                    {
                        runManager->m_indexOfTrialAngle = angleCounter;
                        runManager->m_energyOfGammaOutPerEvent =
                            pStepData->GetPostStepPoint()->GetKineticEnergy();
                        break;
                    }
                }

                // since the interaction we are after happened, we can abort the event
                runManager->getEventManager()->AbortCurrentEvent();
            }
        }
    }

    // If it is not primary gamma or if its energy was reduced already - abort the event
    else
    {
        runManager->getEventManager()->AbortCurrentEvent();
    }
}
```

In such a setup, each Geant4 Run was performed with one of the preset energies (carried in the variable `runManager->m_energyOfPrimaryGammaPerRun`), and for one of the chosen materials. However, the energy distributions for all scattering angles were collected all at once, during the same run. To make sure there is enough meaningful statistics, 500,000,000 events were used in each run; with one gamma shot by the particle gun in each event.

Simulation Results: the Energy Profiles of the Scattered Gamma-Rays

Thus, we collected 24 energy distributions (of the energy of the outgoing gamma in Compton scattering process) for each of the five materials. There was one distribution for each energy of the incoming gamma (100 keV, 200 keV, 400 keV, 800 keV, 1.6 MeV, and 3.2 MeV) and each scattering angle (30 degrees, 60 degrees, 90 degrees, and 120 degrees). The energy profiles were collected as histograms with 0.25 keV bins. The bin width of the histograms and the value of the tolerance constant `runManager->m_angleDeltaPerRun = 0.01 degrees` are related. The tolerance was chosen so that the width of the Compton shelf (without Doppler broadening) for the interactions fitting the condition

```
( (angle >= (trialAngle - runManager->m_angleDeltaPerRun)) &&
  (angle <= (trialAngle + runManager->m_angleDeltaPerRun)) )
```

(where `angle` is the scattering angle in the current interaction and `trialAngle` is one of the scattering angle values for which the distribution is being collected) does not exceed one or two bins. Such choice for the histograms' parameters assured that the width of the energy profiles, collected with LECS turned on, should be attributed to the Doppler broadening effect.

The overview of the distributions collected for the material Silicon is presented in Figures 1 to 4.
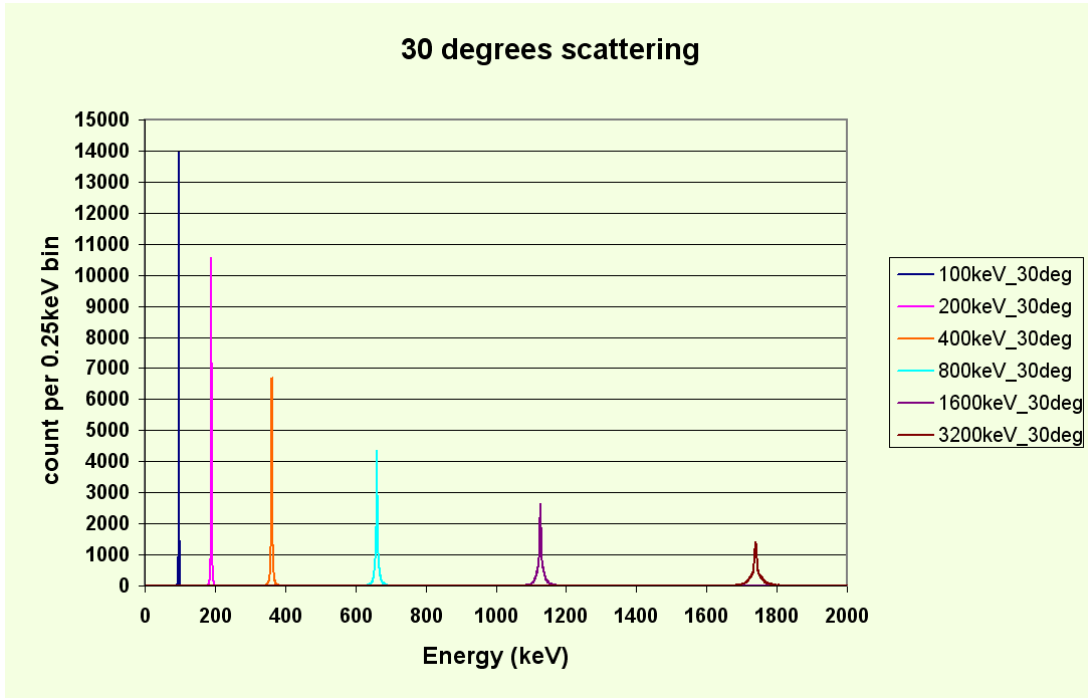

Figure 1. The distributions of the energy of the scattered gamma-ray in Silicon, for several incoming energies. Only Compton interactions with the scattering angles from 29.99 to 30.01 degrees were used. Total number of incoming gamma-rays is 500,000,000 for each energy.
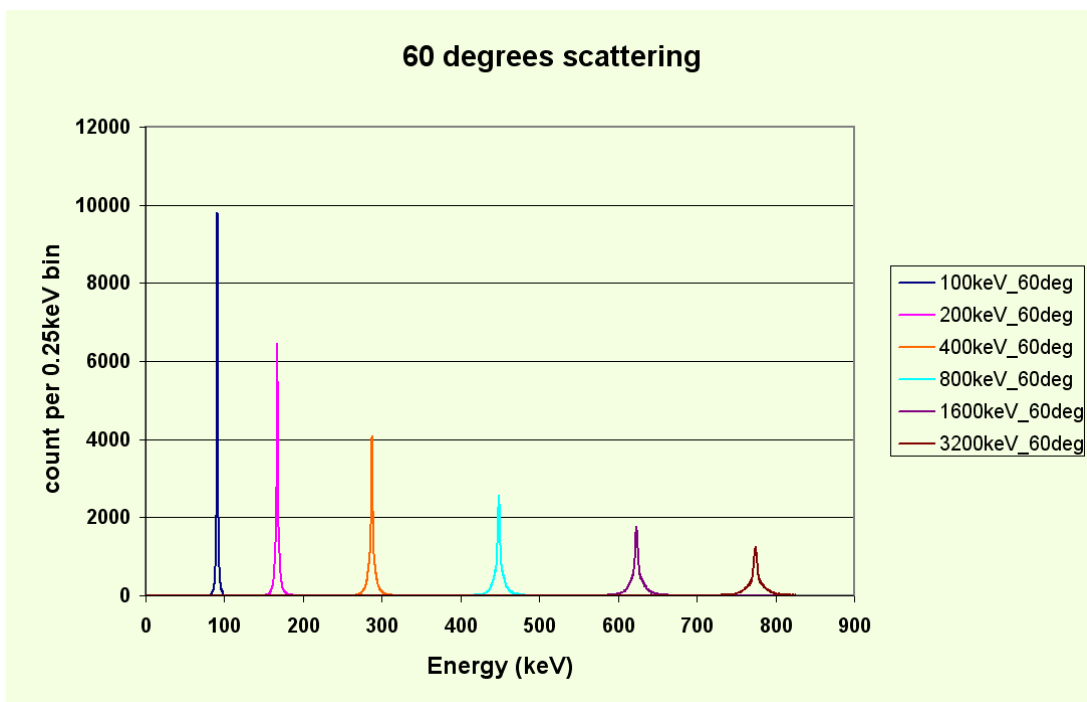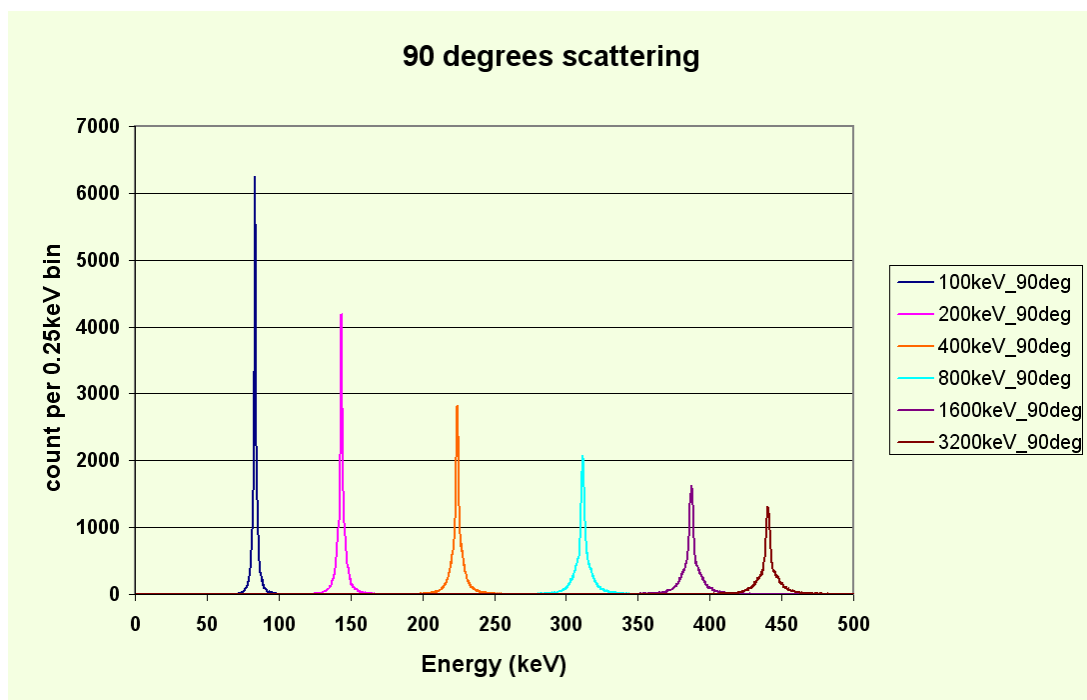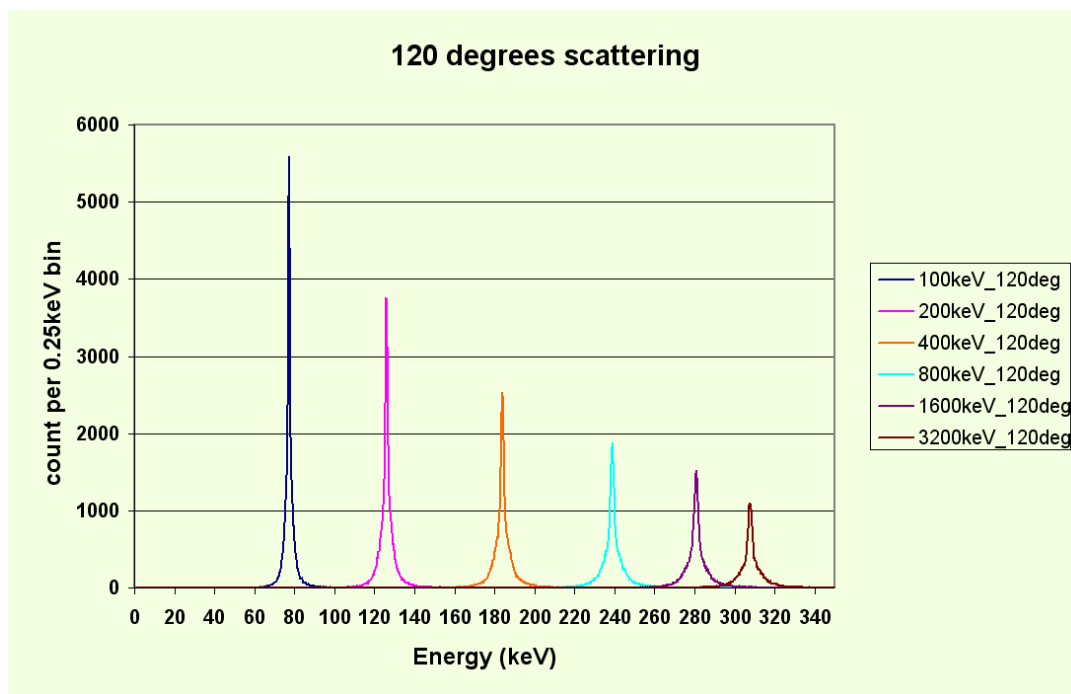
Figure 2. The distributions of the energy of the scattered gamma-ray in Silicon, for several incoming energies. Only Compton interactions with the scattering angles from 59.99 to 60.01 degrees were used. Total number of incoming gamma-rays is 500,000,000 for each energy.

Figure 3. The distributions of the energy of the scattered gamma-ray in Silicon, for several incoming energies. Only Compton interactions with the scattering angles from 89.99 to 90.01 degrees were used. Total number of incoming gamma-rays is 500,000,000 for each energy.

Figure 4. The distributions of the energy of the scattered gamma-ray in Silicon, for several incoming energies. Only Compton interactions with the scattering angles from 119.99 to 120.01 degrees were used. Total number of incoming gamma-rays is 500,000,000 for each energy.

The detailed view of some of the histograms for Silicon and Germanium is given in Figures 5 to 7.
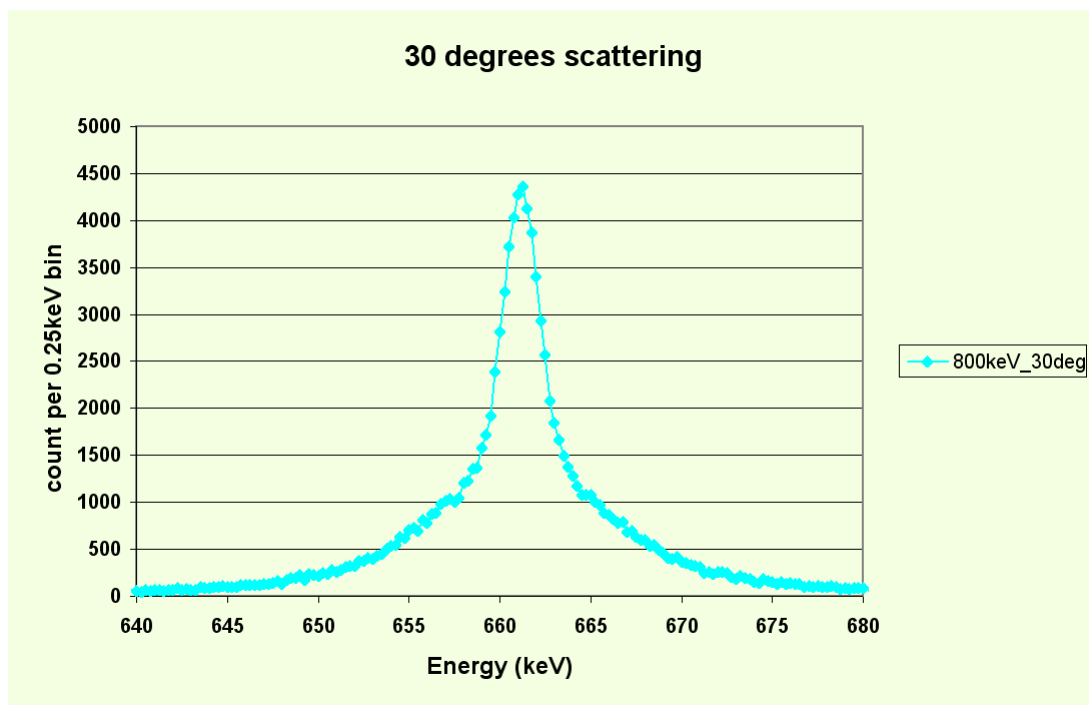

Figure 5. The distribution of the energy of the scattered gamma-ray in Silicon, for the incoming energy of 800keV. Only Compton interactions with the scattering angles from 29.99 to 30.01 degrees were used. Total number of incoming gamma-rays is 500,000,000. Contributions from several different shells are visible.
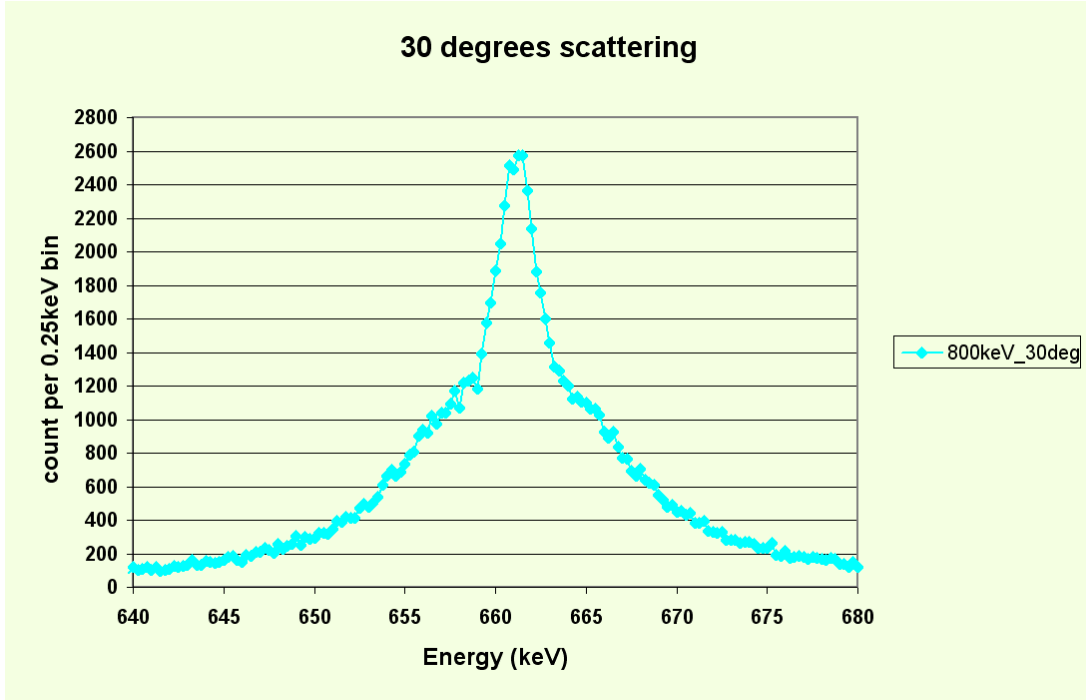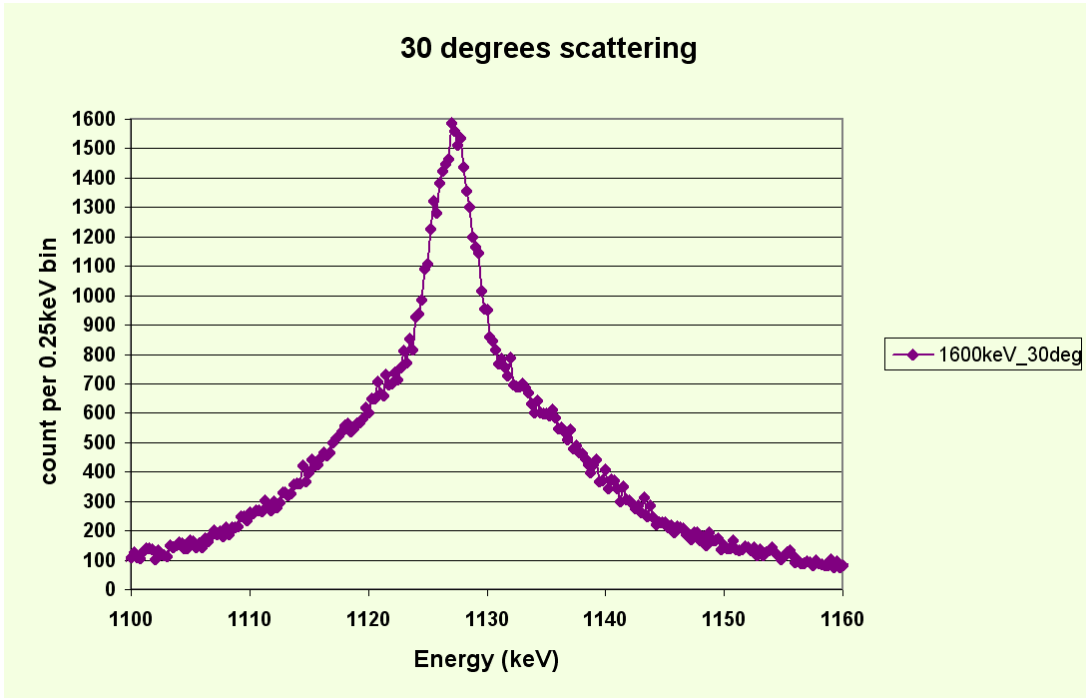
Figure 6. The distribution of the energy of the scattered gamma-ray in Germanium, for the incoming energy of 800keV. Only Compton interactions with the scattering angles from 29.99 to 30.01 degrees were used. Total number of incoming gamma-rays is 500,000,000. Contributions from several different shells are visible.

Figure 7. The distribution of the energy of the scattered gamma-ray in Germanium, for the incoming energy of 1.6MeV. Only Compton interactions with the scattering angles from 29.99 to 30.01 degrees were used. Total number of incoming gamma-rays is 500,000,000. Contributions from several different shells are visible.

The complete set of the collected profiles can be downloaded from [here](#) in the form of Excel files.

Discussion of the Simulated Results

The two most striking features of the simulated distributions are, probably, their considerable width and the fact that they are so heavy-tailed, and, thus, strongly non-Gaussian (due to overlapping contributions from several atomic shells). Despite the latter, the width of such distributions is often measured as FWHM, i.e., Full Width at Half Maximum. This measure is quite misleading, since it tends to grossly underestimate the influence of the Doppler broadening effect on the "accuracy" of the detector. The measure we propose to use is "the full width at 68% containment." This measure gives a better estimate of how much the uncertainty in the energy and angle determination, arising from Doppler broadening effect, influences the accuracy of detectors based on Compton scattering effect.

The dependence of the Doppler broadening, measured (in keV) as the full width of the energy profiles at 68% containment, as a function of the energy of the incoming gamma, is presented in the next four figures, for five different materials. Not all materials are detector-relevant, some of them were chosen to get extreme values of the atomic mass.
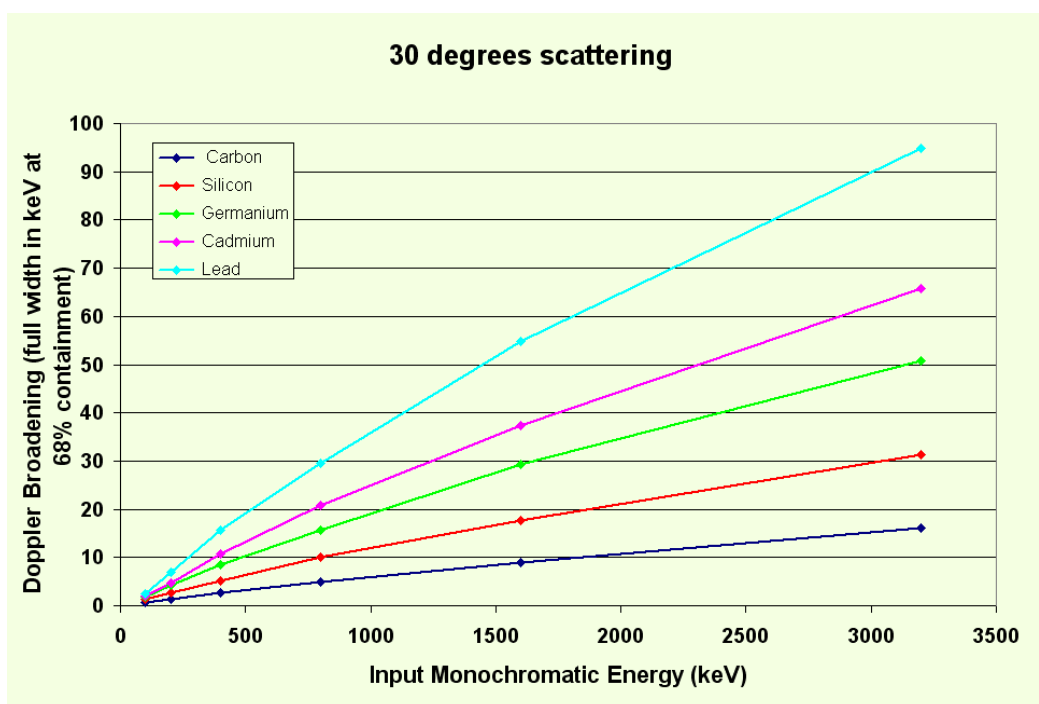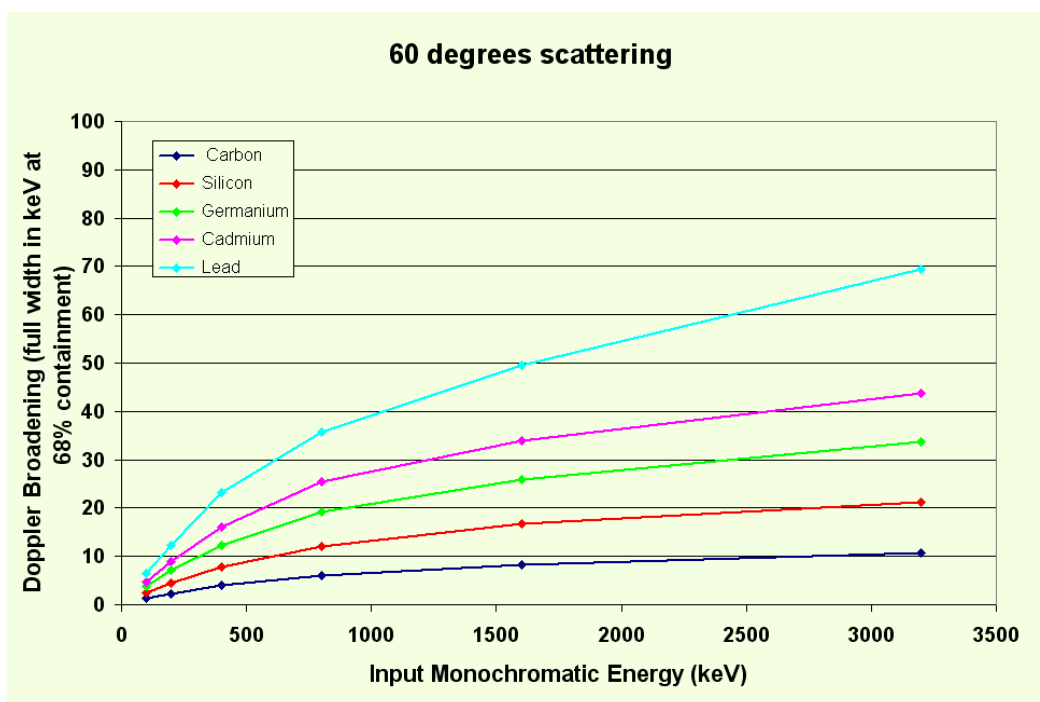

Figure 8. Doppler broadening as a function of the energy of the incoming gamma-ray. Broadening was measured in keV, as the full width at 68% containment for the distributions of the energy of the scattered gamma-ray, for several materials. Only Compton interactions with the scattering angles from 29.99 to 30.01 degrees were used.

Figure 9. Doppler broadening as a function of the energy of the incoming gamma-ray. Broadening was measured in keV, as the full width at 68% containment for the distributions of the energy of the scattered gamma-ray, for several materials. Only Compton interactions with the scattering angles from 59.99 to 60.01 degrees were used.
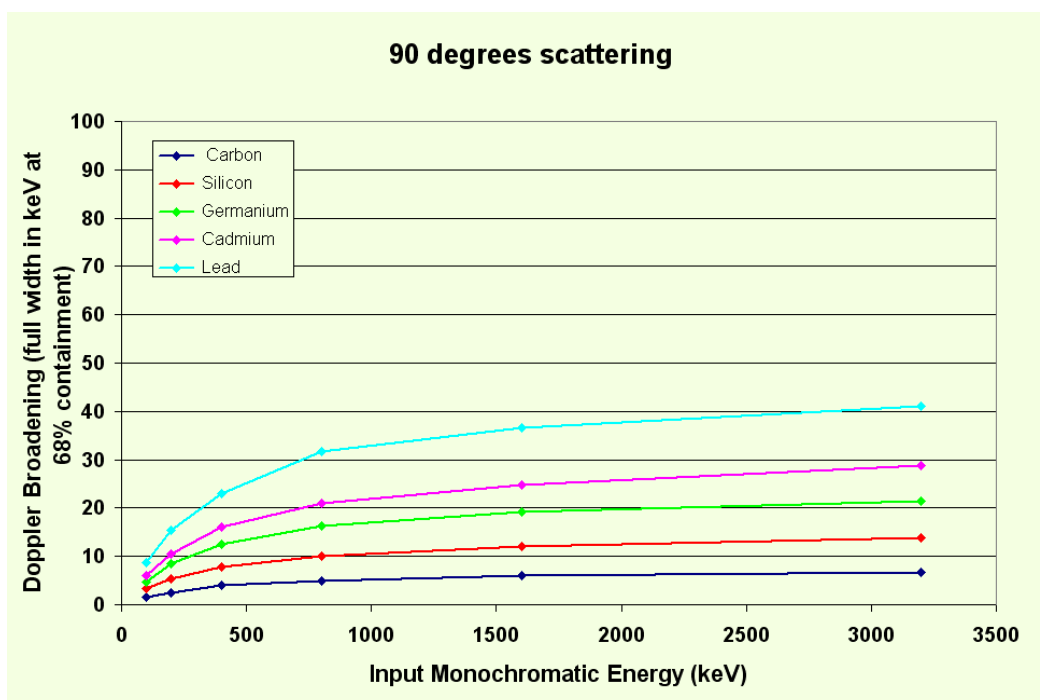

Figure 10. Doppler broadening as a function of the energy of the incoming gamma-ray. Broadening was measured in keV, as the full width at 68% containment for the distributions of the energy of the scattered gamma-ray, for several materials. Only Compton interactions with the scattering angles from 89.99 to 90.01 degrees were used.
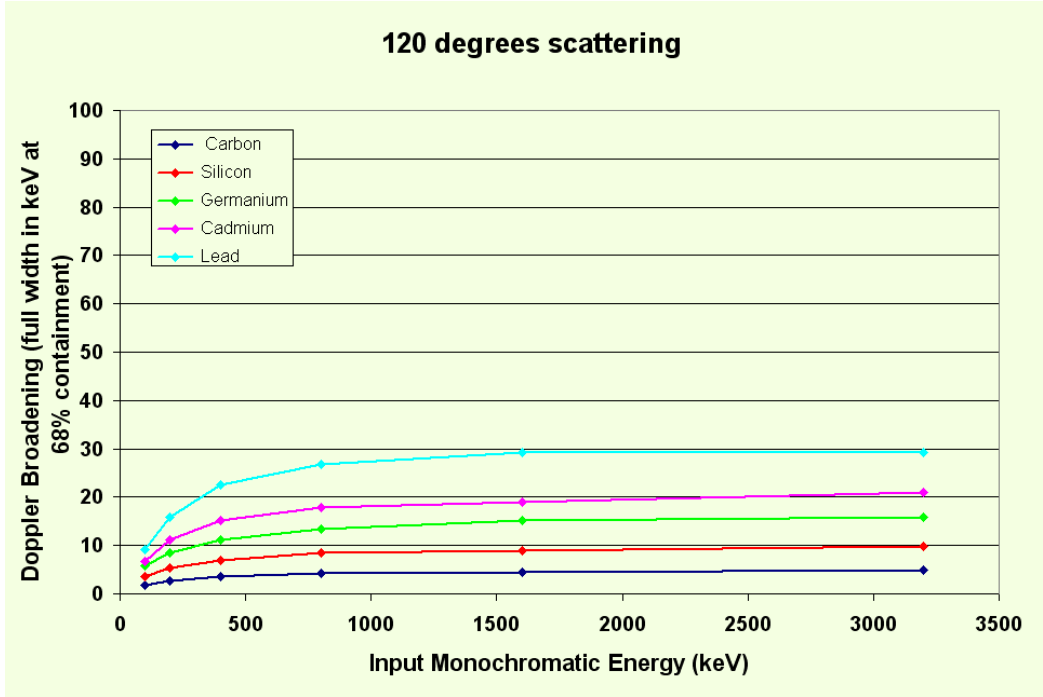
Figure 11. Doppler broadening as a function of the energy of the incoming gamma-ray. Broadening was measured in keV, as the full width at 68% containment for the distributions of the energy of the scattered gamma-ray, for several materials. Only Compton interactions with the scattering angles from 119.99 to 120.01 degrees were used.

Uncertainty in the Value of the Scattering Angle as a Result of Doppler Broadening

In the first part of our testing discussed so far, we studied the energy profiles of the scattered gamma-rays for a given incoming energy and a very narrow range of the scattering angle values. In the second part of our testing, we inverted the setup. This time, we also used the monochromatic beam of incoming gamma-rays, but studied the profiles of the scattering angle values for a very narrow range of the energy values of the scattered gamma-rays.

Simulation Setup

The set of energies of the incoming gamma-ray used in the first part of the testing was also used in the second part: 100 keV, 200 keV, 400 keV, 800 keV, 1.6 MeV, and 3.2 MeV. The same set of materials was used: Carbon, Silicon, Germanium, Cadmium, and Lead. We wanted to study angular distributions of the scattered gamma-rays centered at the same scattering angles as used in the first part of the simulation: 30 degrees, 60 degrees, 90 degrees, and 120 degrees. To accomplish this, we had to collect the histograms of the scattering angle for the scattering energy that, for a pure Compton effect (no Doppler broadening) would result in the preset scattering angle. For example, for the incoming energy of 100 keV and the histogram centered at the scattering angle of 30 degrees, we had to collect Compton interactions with the scattering energy of 97.44517 plus/minus some very small value (called `runManager->m_energyDeltaPerRun`) . For each incoming energy, and each preset scattering angle (30, 60, 90, or 120 degrees), the corresponding angle of the scattering gamma-ray was computed using pure Compton equation. The value `runManager->m_energyDeltaPerRun` was set to 0.015 keV, which allowed to have the bin width of the histogram of 0.02 degree.

The relevant part of the `main()` code is shown below. As it is clear from this code, there were 2,000,000,000 gamma-ray used to collect statistics for each energy value.

```
    // The energies of the peaks: get it off the equation
    for (int energyCounter = 0; energyCounter < N_ENERGIES; ++energyCounter)
    {
        double energy = 100.* keV * pow(2.0, energyCounter);

        for (int angleCounter = 0; angleCounter < N_ANGLES; ++angleCounter)
        {
            double angle = double(30 + 30 * angleCounter);

            double energyOut = 1./(1./energy - (cos(angle*deg) - 1)/0.511);    // in MeV
            runManager->m_energiesOfInterest[angleCounter][energyCounter] = energyOut;
        }
    }

    // Run it
    for (int energyCounter = 0; energyCounter < N_ENERGIES; ++energyCounter)
    {
        runManager->m_energyOfPrimaryGammaPerRun = 100.* keV * pow(2.0, energyCounter);

        for (int angleCounter = 0; angleCounter < N_ANGLES; ++angleCounter)
        {
            int angleInt = 30 + 30 * angleCounter;
        }

        runManager->BeamOn(static_cast<int>(2.e9));
    }
```

The portion of the user supplied stepping action class where the collection criteria are applied, can be found in the following code box:

```
// ------------------------------------------------------------------------
// Virtual method of the base class G4UserSteppingAction.
// This method is invoked at the end of each step.

void
SteppingAction::
UserSteppingAction(
    G4Step const* pStepData)
{
    // Get run manager pointer. Run manager keeps gun setup information and all statistical results
    RunManager* runManager = static_cast<RunManager*>(G4RunManager::GetRunManager());

    G4Track const* pTrack = pStepData->GetTrack();

    // If this is the primary gamma, check it out
    if( (G4Gamma::Gamma()== pTrack->GetDefinition()) && (pTrack->GetParentID() == 0) &&
        (pStepData->GetPreStepPoint()->GetKineticEnergy() == runManager->m_energyOfPrimaryGammaPerRun) )
    {
        G4String processName = ' ';
        G4VProcess const* processStep = pStepData->GetPostStepPoint()->GetProcessDefinedStep();
        if(processStep)
        {
            processName = processStep->GetProcessName();
            G4double energy = pStepData->GetPostStepPoint()->GetKineticEnergy();

            if ( (processName == "LowEnCompton") || (processName == "G4LECSComp1.01") )
            {
                for (int angleCounter = 0; angleCounter < N_ANGLES; ++angleCounter)
                {
                    G4double trialEnergy = runManager->m_energiesOfInterest
                        [angleCounter][runManager->runID()];

                    if ( (energy >= (trialEnergy - runManager->m_energyDeltaPerRun)) &&
                         (energy <= (trialEnergy + runManager->m_energyDeltaPerRun)) )
                    {
                        runManager->m_indexOfTrialAngle = angleCounter;

                        G4ThreeVector const& before = pStepData->GetPreStepPoint()->GetMomentumDirection();
                        G4ThreeVector const& after = pStepData->GetPostStepPoint()->GetMomentumDirection();
```

12

```
                    runManager->m_angleOfGammaOutPerEvent = after.angle(before);
                    break;
                }
            }

            // since the interaction we are after happened, we can abort the event
            runManager->getEventManager()->AbortCurrentEvent();
        }
        else if (energy != runManager->m_energyOfPrimaryGammaPerRun)
        {
            runManager->getEventManager()->AbortCurrentEvent();
        }
    }
}

// If it is not primary gamma or if its energy was reduced already - abort the event
else
{
    runManager->getEventManager()->AbortCurrentEvent();
}
}
```

Simulation Results: the Profiles of the Scattering Angle for a Fixed Energy of the Scattered Gamma-Ray

For each tested material, 24 profiles of the scattering angle were collected: one for each of the six values of the incoming energy and each value of the scattering angle that would have been observes if there were no Doppler broadening effect. The overview of the profiles for Silicon is presented in Figures 12 to 17.
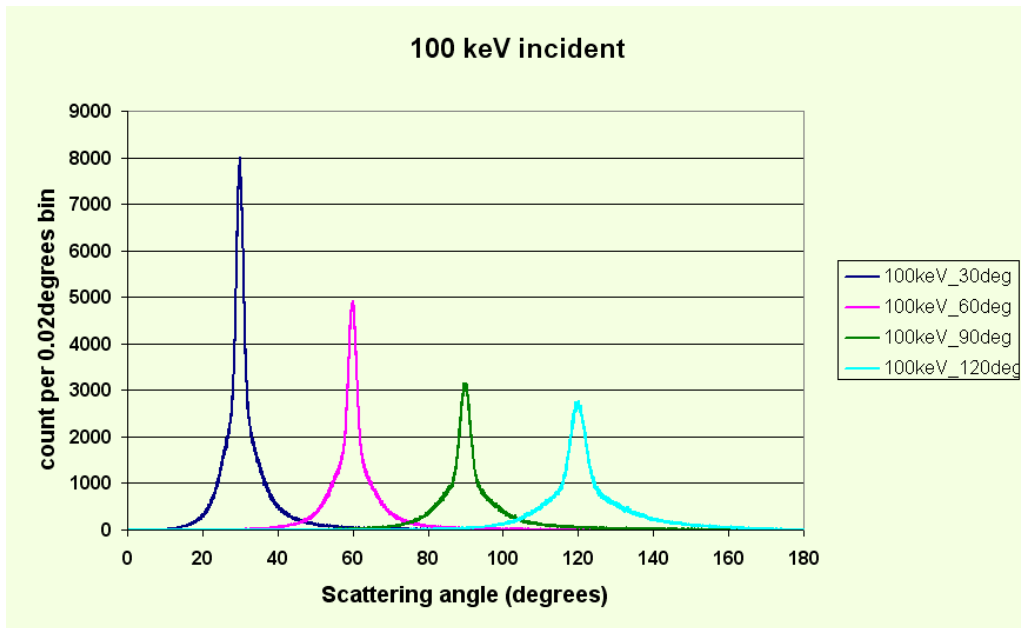

Figure 12. The distributions of the scattering angle of the gamma-ray in Silicon, for the incoming energy of 100 keV. Only Compton interactions with the energy of the scattered gamma ray close to the energy corresponding to the scattering angle of 30, 60, 90, or 120 degrees in the absence of Doppler broadening were used. The "close" was defined as being within 0.015 keV of the exact value. Total number of incoming gamma-rays is 2 billion.
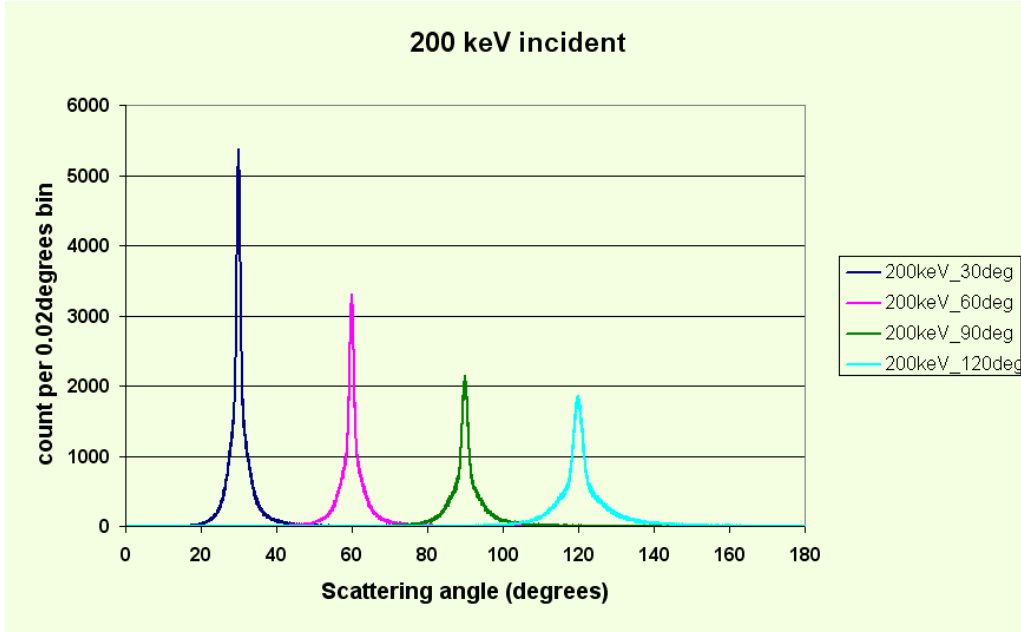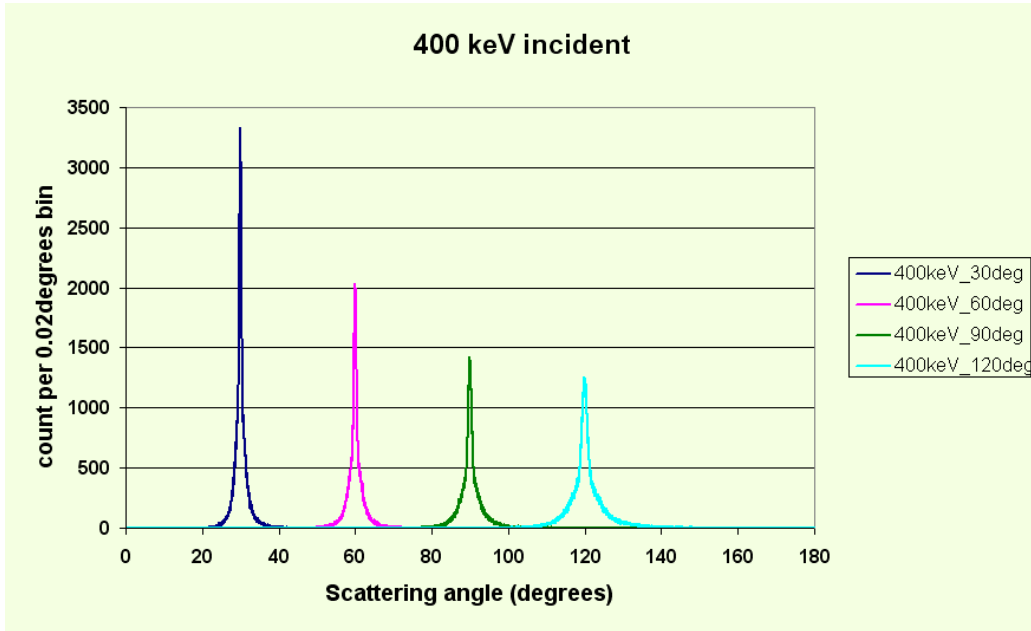
Figure 13. The distributions of the scattering angle of the gamma-ray in Silicon, for the incoming energy of 200 keV. Only Compton interactions with the energy of the scattered gamma ray close to the energy corresponding to the scattering angle of 30, 60, 90, or 120 degrees in the absence of Doppler broadening were used. The "close" was defined as being within 0.015 keV of the exact value. Total number of incoming gamma-rays is 2 billion.
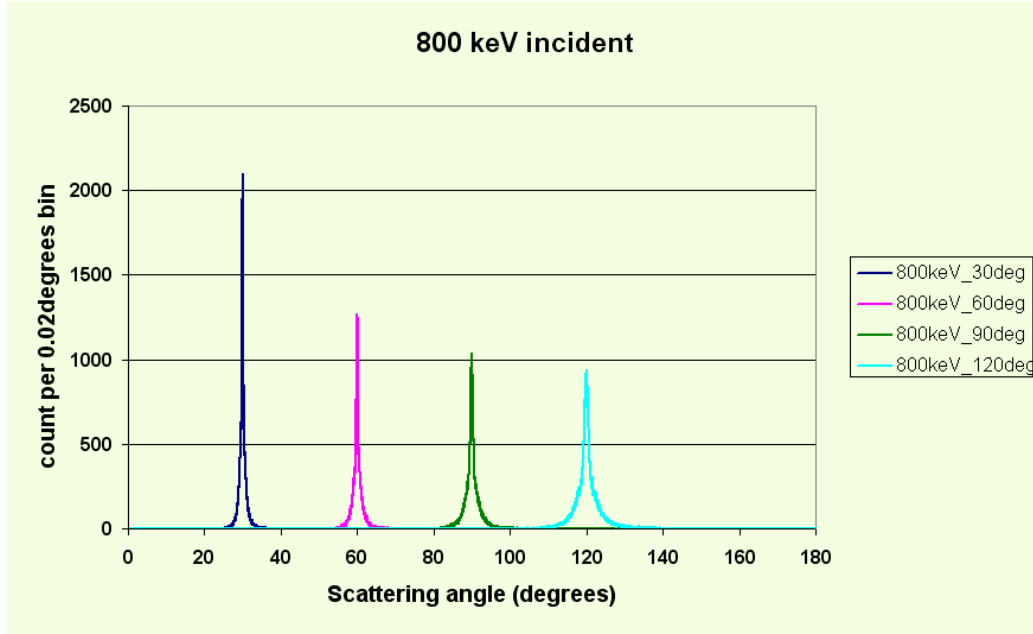

Figure 14. The distributions of the scattering angle of the gamma-ray in Silicon, for the incoming energy of 400 keV. Only Compton interactions with the energy of the scattered gamma ray close to the energy corresponding to the scattering angle of 30, 60, 90, or 120 degrees in the absence of Doppler broadening were used. The "close" was defined as being within 0.015 keV of the exact value. Total number of incoming gamma-rays is 2 billion.
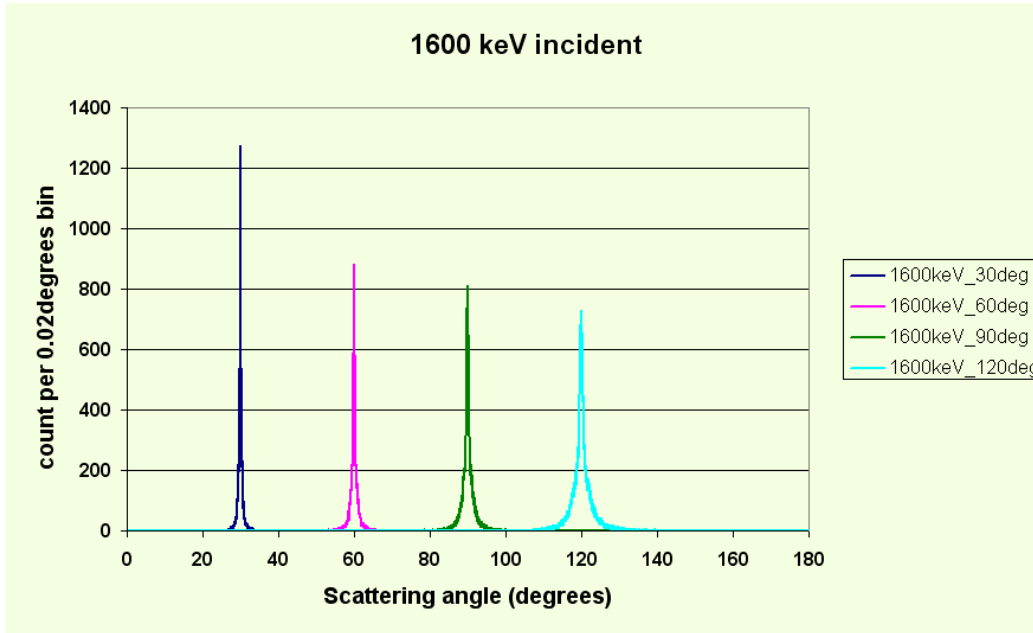
14

Figure 15. The distributions of the scattering angle of the gamma-ray in Silicon, for the incoming energy of 800 keV. Only Compton interactions with the energy of the scattered gamma ray close to the energy corresponding to the scattering angle of 30, 60, 90, or 120 degrees in the absence of Doppler broadening were used. The "close" was defined as being within 0.015 keV of the exact value. Total number of incoming gamma-rays is 2 billion.
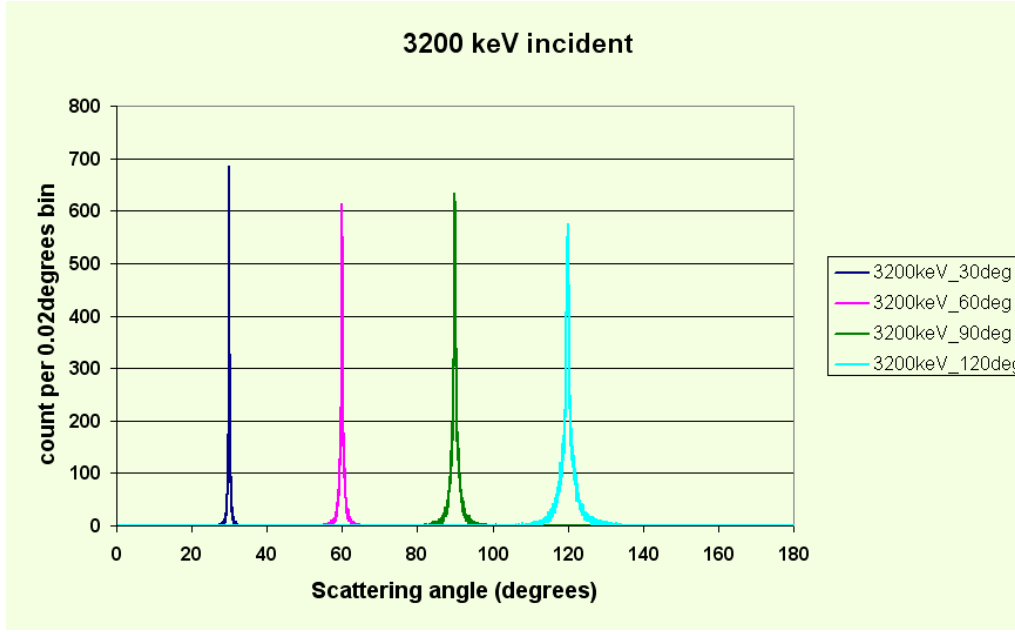

Figure 16. The distributions of the scattering angle of the gamma-ray in Silicon, for the incoming energy of   1.6 MeV. Only Compton interactions with the energy of the scattered gamma ray close to the energy corresponding to the scattering angle of 30, 60, 90, or 120 degrees in the absence of Doppler broadening were used. The "close" was defined as being within 0.015 keV of the exact value. Total number of incoming gamma-rays is 2 billion.
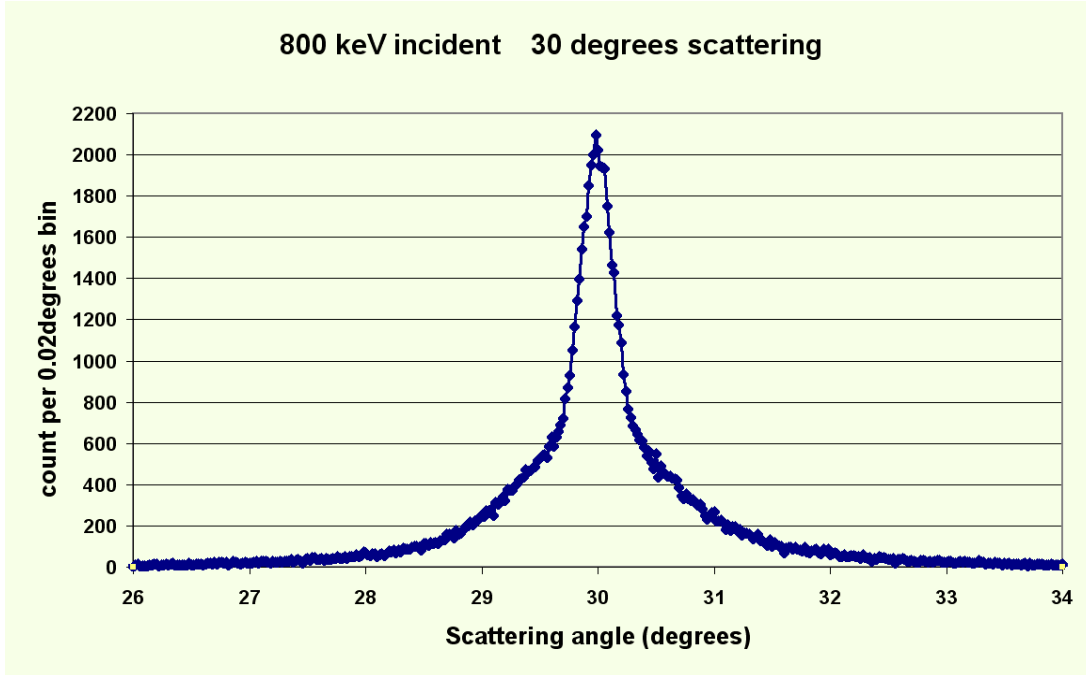
Figure 17. The distributions of the scattering angle of the gamma-ray in Silicon, for the incoming energy of 3.2 MeV. Only Compton interactions with the energy of the scattered gamma ray close to the energy corresponding to the scattering angle of 30, 60, 90, or 120 degrees in the absence of Doppler broadening were used. The "close" was defined as being within 0.015 keV of the exact value. Total number of incoming gamma-rays is 2 billion.

Figure 18. The distributions of the scattering angle of the gamma-ray in Silicon, for the incoming energy of 800 keV. Only Compton interactions with the energy of the scattered gamma ray close to the energy corresponding to the scattering angle of 30 degrees in the absence of Doppler broadening were used. The "close" was defined as being within 0.015 keV of the exact value. Total number of incoming gamma-rays is 2 billion.

The zoomed in view of one of the distributions is shown in Figure 18. The contribution from several atomic shells is clearly seen, and it is again obvious that the width of such a distribution should not be measured as FWHM.

The complete set of the collected profiles can be downloaded from <u>here</u> in the form of Excel files.

Discussion of the Simulated Results

The Doppler broadening, measured in degrees, as the full width of the distribution of the scattering angle at 68% containment, as a function of the energy of the incoming gamma, is presented in the next four figures. For low incident energies and higher Z values, the uncertainty of scattering angle (due to Doppler broadening), for a given scattering energy, is very large. Even for low values of Z (such materials as Silicon and Germanium), the uncertainty in the scattering angle is very significant at low energies, even for forward scattering.
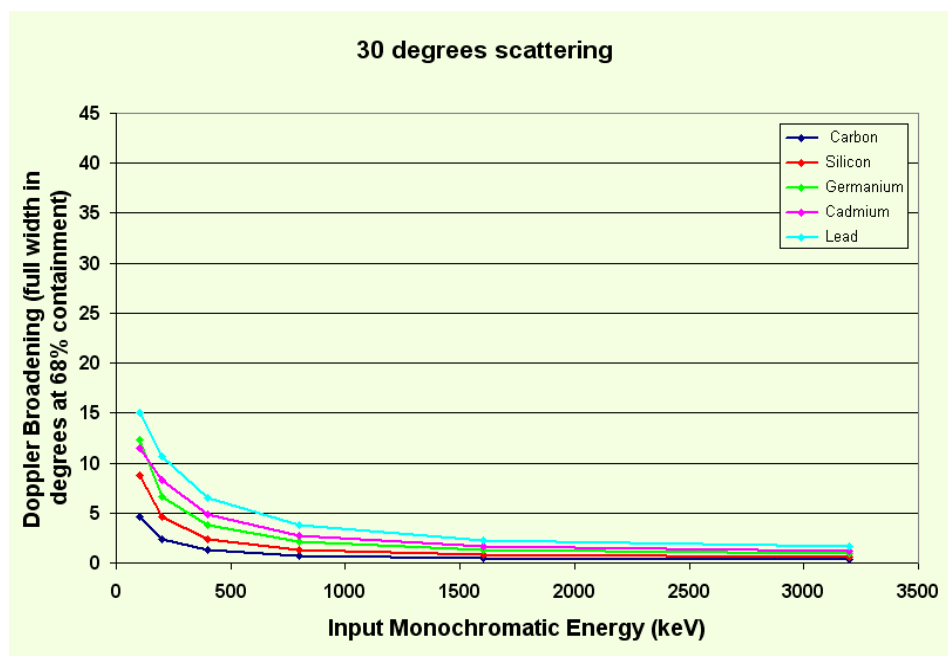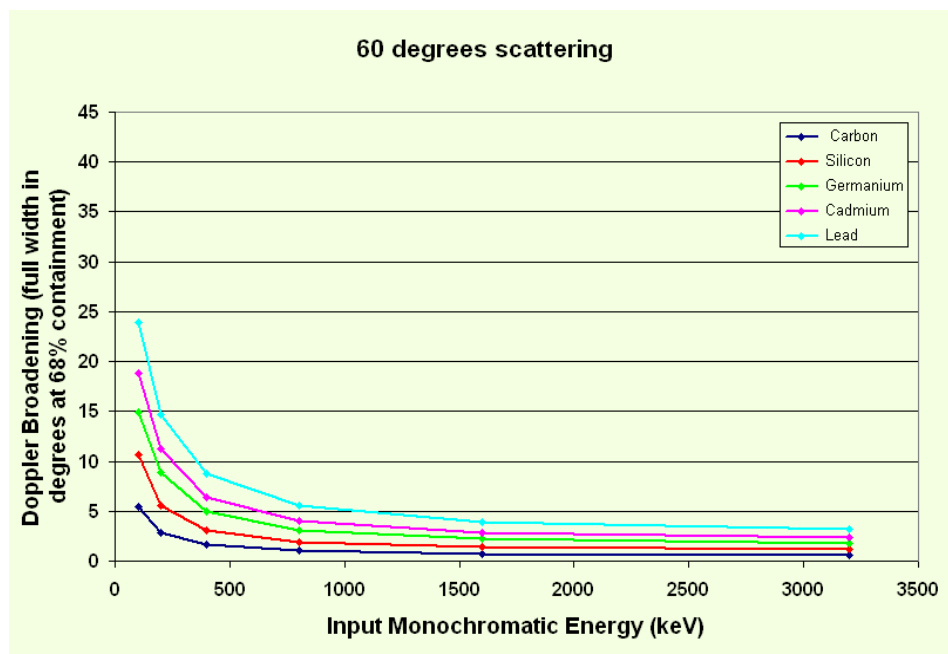

Figure 19. Doppler broadening as a function of the energy of the incoming gamma-ray. Broadening was measured in degrees, as the full width at 68% containment for the distributions of the scattering angle of the scattered gamma-ray, for several materials. Only Compton interactions with the energy of the scattered gamma ray close to the energy corresponding to the scattering angle of 30 degrees in the absence of Doppler broadening were used. The "close" was defined as being within 0.015 keV of the exact value.

Figure 20. Doppler broadening as a function of the energy of the incoming gamma-ray. Broadening was measured in degrees, as the full width at 68% containment for the distributions of the scattering angle of the scattered gamma-ray, for several materials. Only Compton interactions with the energy of the scattered gamma ray close to the energy corresponding to the scattering angle of 60 degrees in the absence of Doppler broadening were used. The "close" was defined as being within 0.015 keV of the exact value.
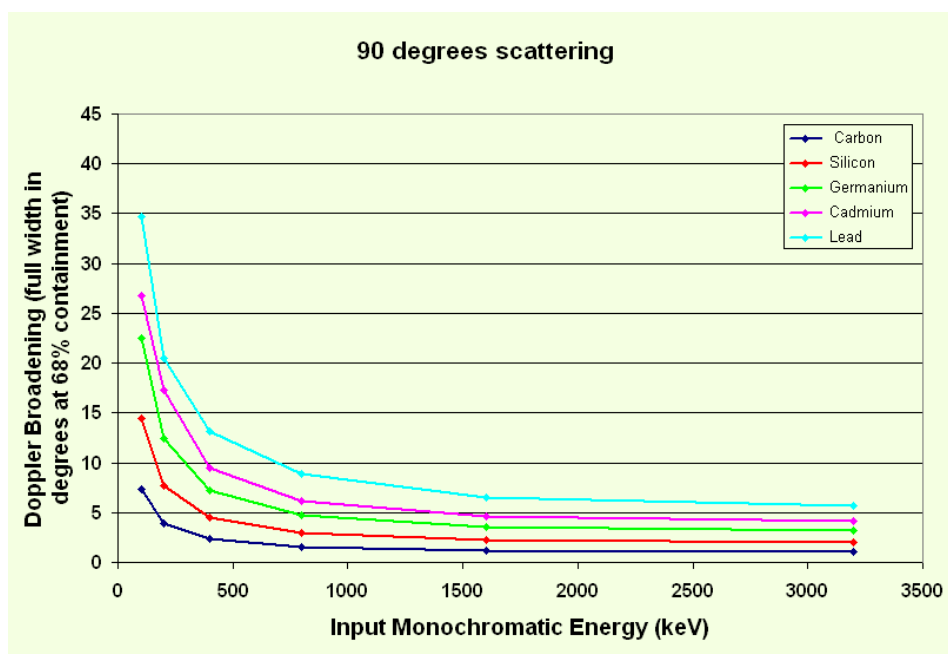

Figure 21. Doppler broadening as a function of the energy of the incoming gamma-ray. Broadening was measured in degrees, as the full width at 68% containment for the distributions of the scattering angle of the scattered gamma-ray, for several materials. Only Compton interactions with the energy of the scattered gamma ray close to the energy corresponding to the scattering angle of 90 degrees in the absence of Doppler broadening were used. The "close" was defined as being within 0.015 keV of the exact value.
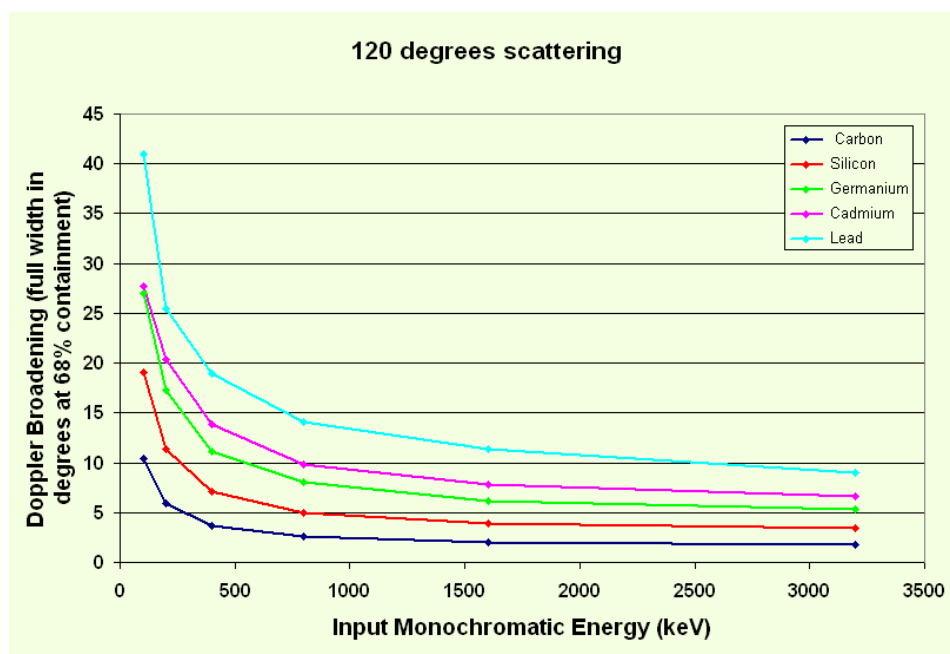
Figure 22. Doppler broadening as a function of the energy of the incoming gamma-ray. Broadening was measured in degrees, as the full width at 68% containment for the distributions of the scattering angle of the scattered gamma-ray, for several materials. Only Compton interactions with the energy of the scattered gamma ray close to the energy corresponding to the scattering angle of 120 degrees in the absence of Doppler broadening were used. The "close" was defined as being within 0.015 keV of the exact value.

Shell effects

The LECS code allows one not only to see the general trends, but also to see the smaller features of the Doppler broadening. Since the code takes into account contribution of several atomic shells, one can observe shell effect in the results. For example, we can see the shell effect in the distributions of the scattering angle for a fixed energy of the scattered gamma-ray.

The curves for Germanium (Z=32) and Cadmium (Z=48) cross each other in Figure 19, while all other curves seem to show monotonic behavior: with increase of Z, the width of the distribution increases. After checking the table of the binding energies for various shells for Ge and Cd (Lederer and Shirley, 1978), we find that the binding energy for L1 shell of Cd is 4.018 keV, and the binding energy of L1 shell of Ge is just 1.413 keV. On the other hand, the 100keV photon looses 2.555 keV during a 30 degrees scatter, thus supplying plenty of energy for the release of an electron from L1 shell of Germanium, but not enough to release an electron from the L1 shell of Cadmium. Hence, more shell electrons (with various binding energies) are "available" for release by a 100 keV photon hitting a Ge atom, than hitting a Cd atom. This results in a broader distribution for Ge than Cd.

The results of the similar effect for two more pairs of Z values is demonstrated in Figure 23. To make demonstration cleaner, we chose the pairs of Z values that differ by only one unit.
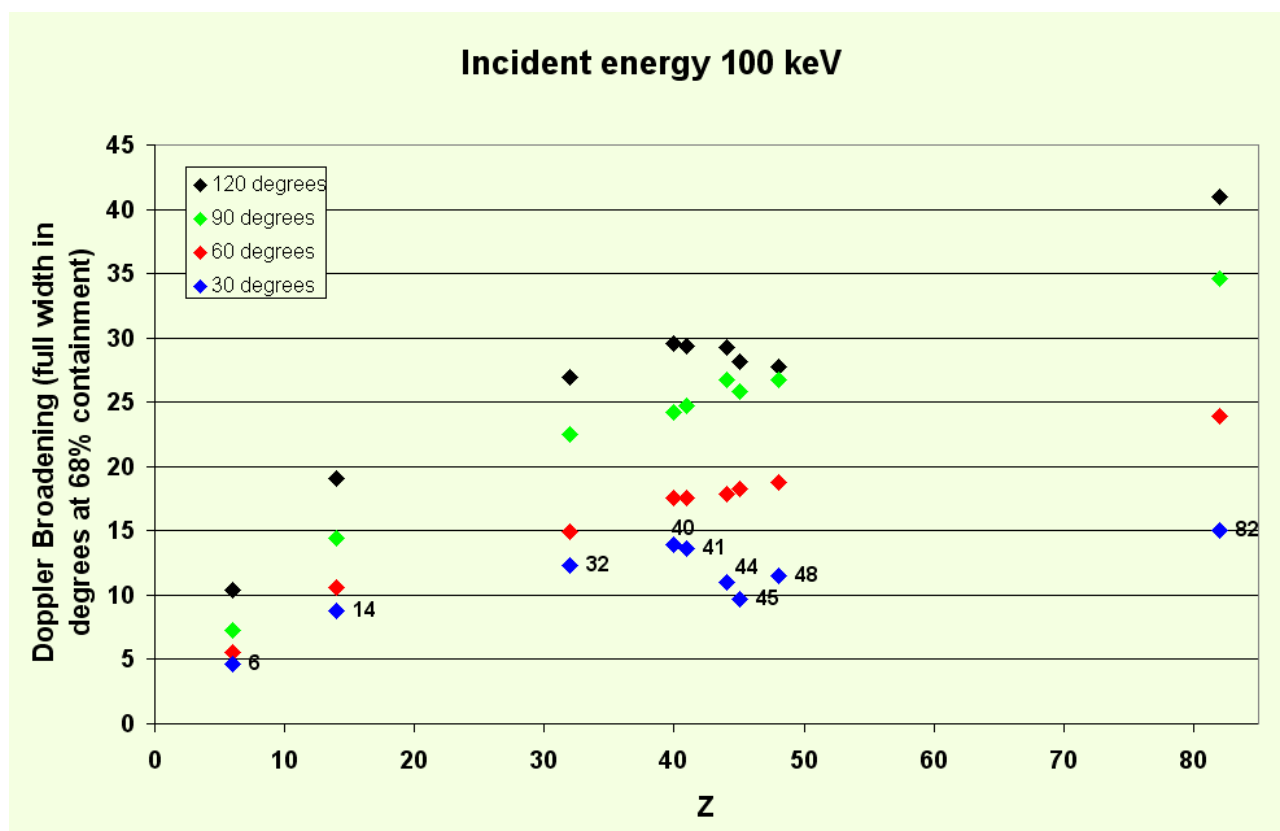
Figure 23. Doppler broadening as a function of the atomic mass: the effect of shells. Broadening was measured in degrees, as the full width at 68% containment for the distributions of the scattering angle of the scattered gamma-ray. Only interactions with the energy of the scattered gamma ray close to the energy corresponding to the scattering angle of 30, 60, 90, or 120 degrees in the absence of Doppler broadening were used. The "close" was defined as being within 0.015 keV of the exact value.

Indeed, the binding energy of the L1 shell of Zirconium (Z=40) is 2.534 keV, which is below the value lost by a 100 keV photon in a Compton interaction with the scattering of 30 degrees (which is 2.555 keV). On the other hand, the binding energy of the L1 shell in Niobium (Z=41) is 2.695 keV, which makes it unavailable for the 30 degrees scatter of a 100 keV photon. As a result, the Doppler broadening effect (at 100 keV, 30 degrees scatter) is more pronounced for Zirconium than for Niobium.

The pair of elements Ruthenium (Z=44) and Rhodium (Z=45) presents similar behavior for the scattering angle of 120 degrees, which can be explained by the values of the binding energies of their K shells. For the Ruthenium, this value is 22.117 keV, and for Rhodium it is 23.220 keV. The energy lost by a 100 keV photon during 120 degrees Compton scatter is 22.693 keV, which makes K shell of Rhodium unavailable for such a scatter, while the K shell of Ruthenium remains available.

Measures of Doppler Broadening

The results of our testing of the LECS package show the dangers of attempts to measure the degree of Doppler broadening by using just one number. Given that the distributions of the scattering angle for a given scattering energy is a very heavy-tailed one, because it consists of several overlapping contributions from several shells

20

(and from several elements - in composite materials), measures of the width of such distributions using one number can be misleading. Especially dangerous is FWHM. Detailed view of a distribution, such as in Figure 18, shows that FWHM measures only contribution from one (or just a few) shells, and does not reflect the heavy tailed nature of the distributions. Thus, if the goal is to represent the width of the distribution using just one number, the "containment" measure seems to be a more appropriate one. We usually use 68% containment. Two other "containment" measures (50% and 80%), along with FWHM, are shown in the Figures 24 to 27 for some commonly used materials.
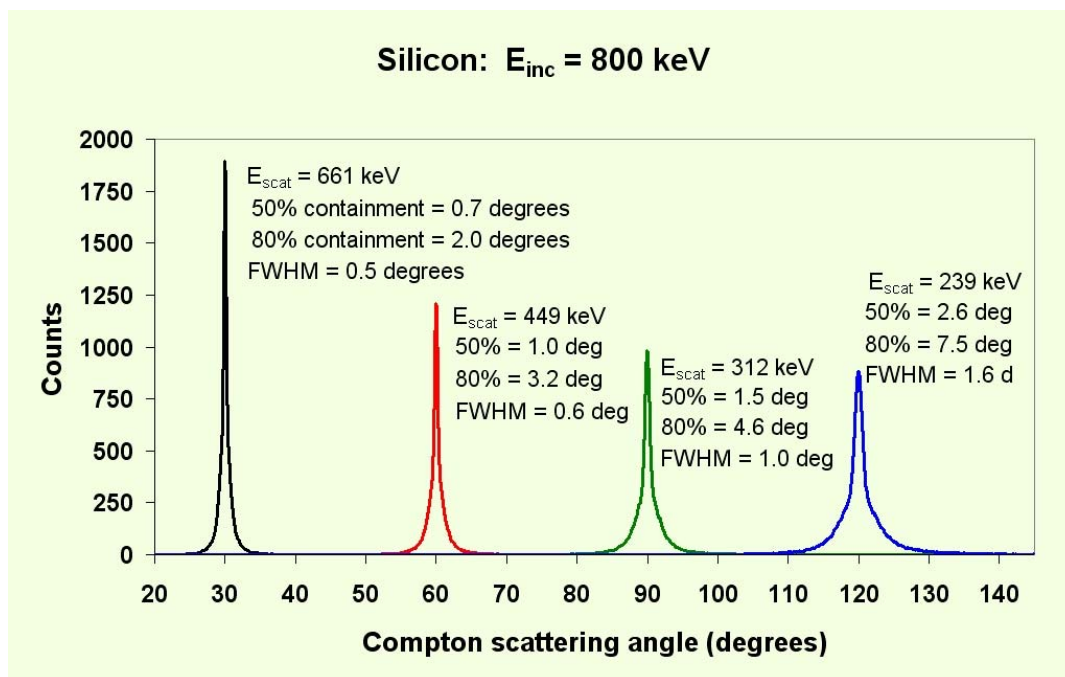

Figure 24. The distributions of the scattering angle of the gamma-ray in Silicon, for the incoming energy of 800 keV (similar to Figure 16). For each scattering angle, the following values are given: the energy of the scattered gamma-ray, the width of the distribution measured 50% and 80% containment, and FWHM.
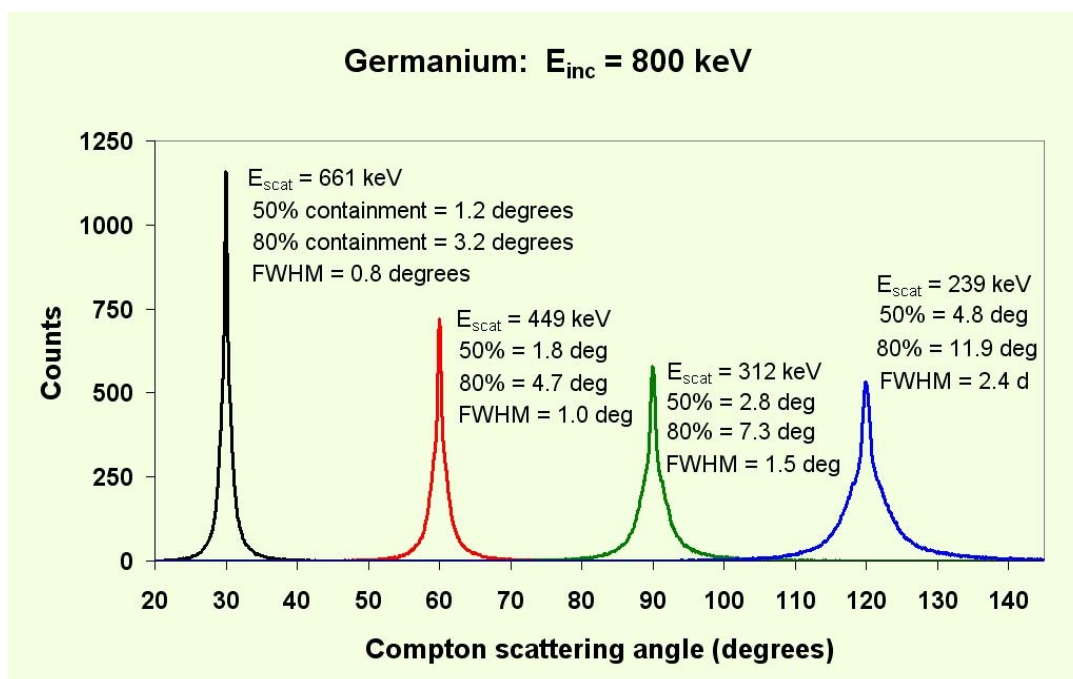
Figure 25. The distributions of the scattering angle of the gamma-ray in Germanium, for the incoming energy of 800 keV (similar to Figure 16). For each scattering angle, the following values are given: the energy of the scattered gamma-ray, the width of the distribution measured 50% and 80% containment, and FWHM.
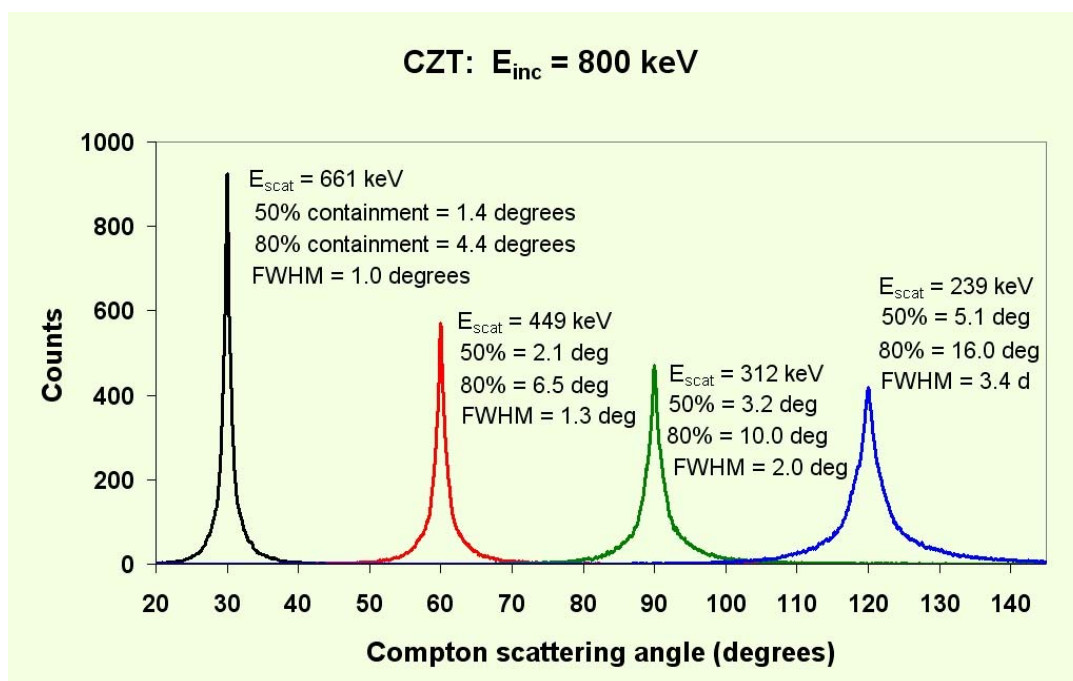

Figure 26. The distributions of the scattering angle of the gamma-ray in CZT, for the incoming energy of 800 keV (similar to Figure 16). For each scattering angle, the following values are given: the energy of the scattered gamma-ray, the width of the distribution measured 50% and 80% containment, and FWHM.
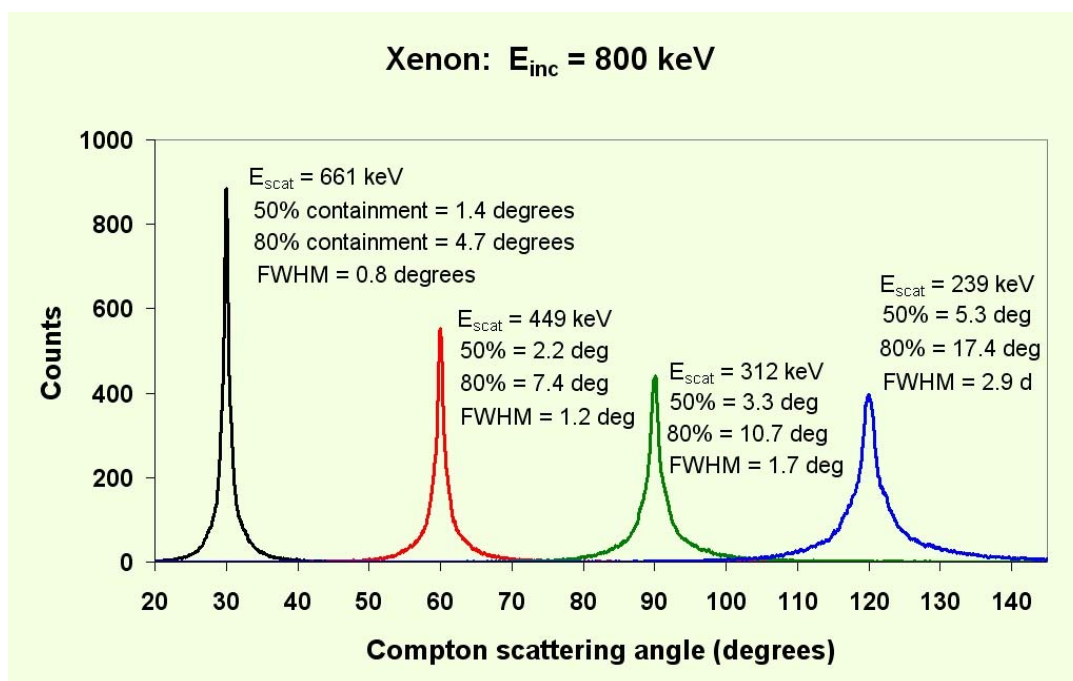
Figure 27. The distributions of the scattering angle of the gamma-ray in Xenon, for the incoming energy of 800 keV (similar to Figure 16). For each scattering angle, the following values are given: the energy of the scattered gamma-ray, the width of the distribution measured 50% and 80% containment, and FWHM.

One more comparison of the two measures—68% containment versus the FWHM—is presented in Figures 28 and 29.
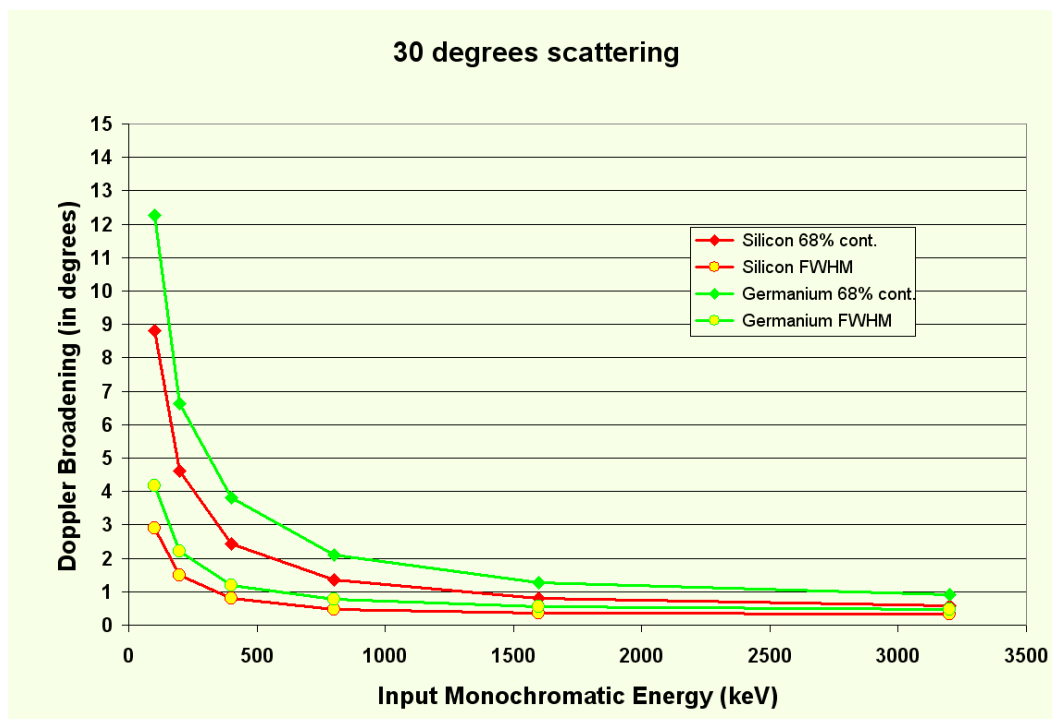

Figure 28. Doppler broadening as a function of the energy of the incoming gamma-ray. Broadening was measured in degrees, as the full width at 68% containment, and as FWHM, for Silicon and Germanium.
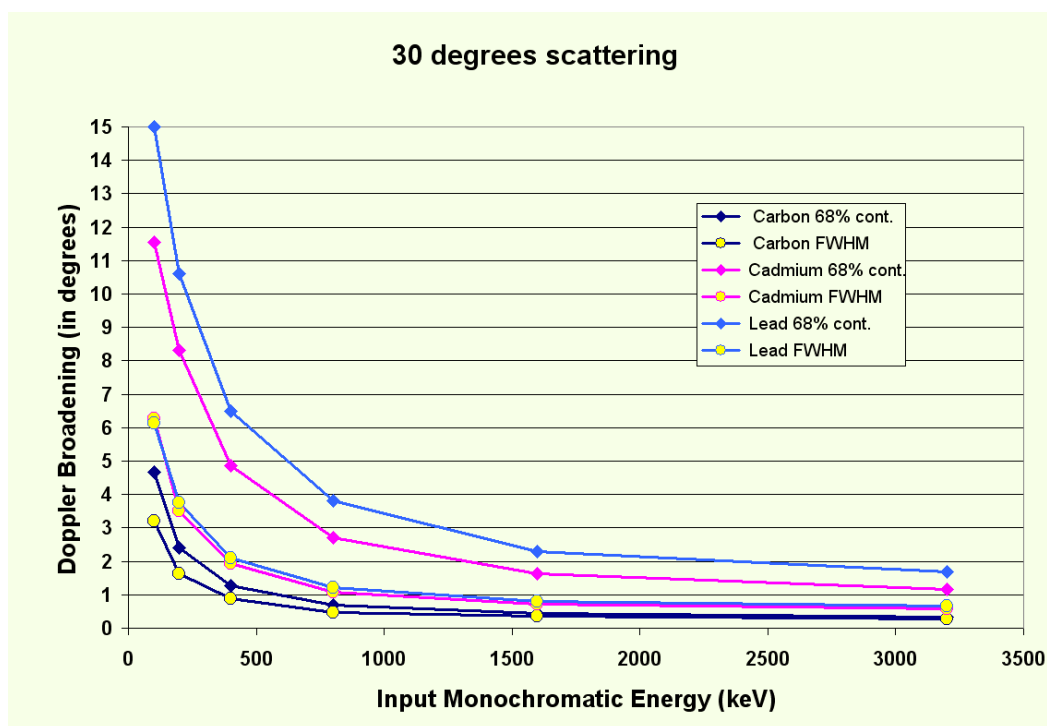
Figure 29. Doppler broadening as a function of the energy of the incoming gamma-ray. Broadening was measured in degrees, as the full width at 68% containment, and as FWHM, for Carbon, Cadmium and Lead.

Comparison of LECS to Analytical Derivations

Carolyn Lehner, graduate student at the Department of Nuclear Engineering and Radiological Sciences at the University of Michigan, compared the results presented here with the analytical expressions (see references below, in the text of Lehner's notes) and some tabulated data. Her results (for Cadmium) are presented in Figure 30.
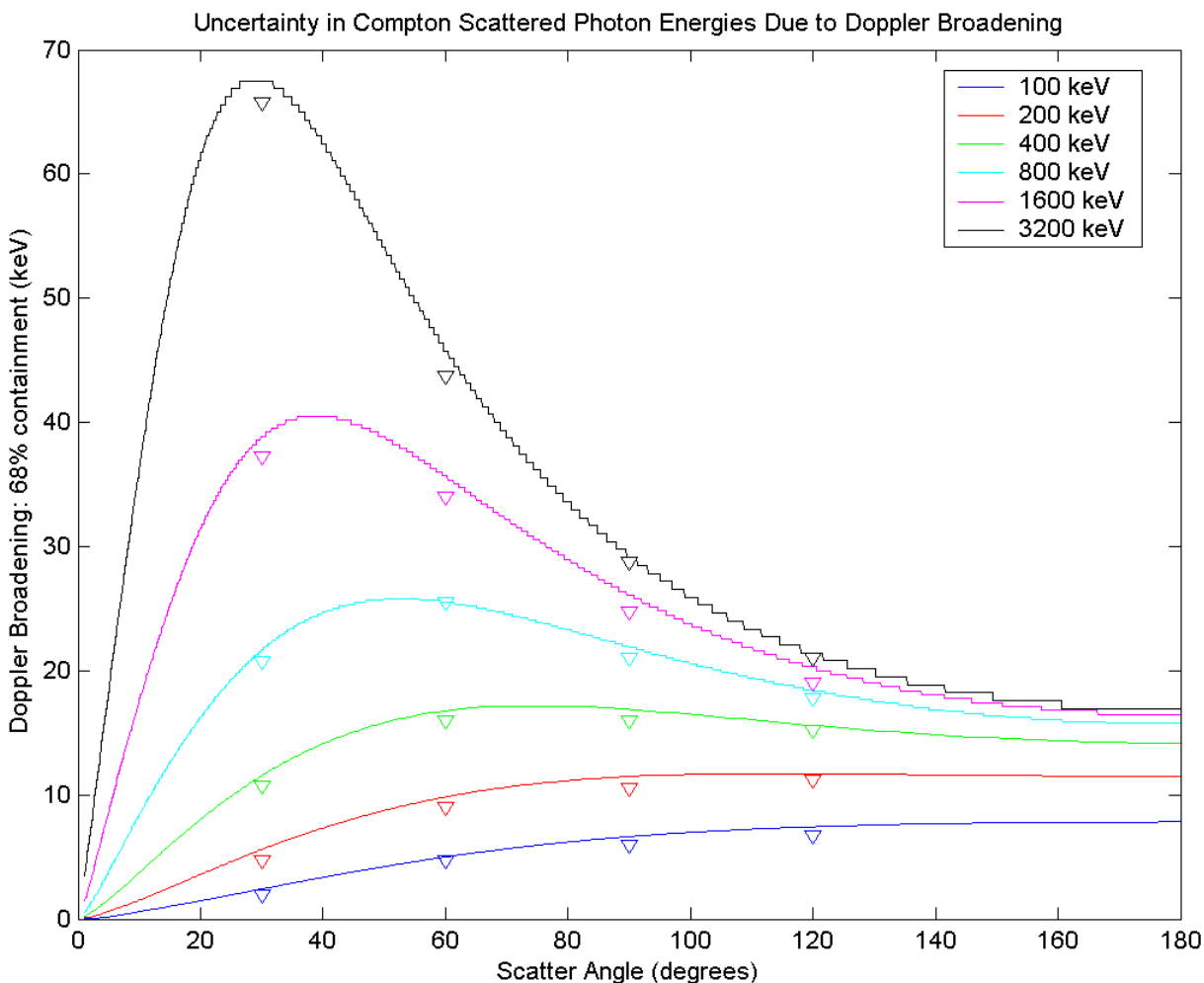
Figure 30. Uncertainties in Compton scattered energies due to Doppler broadening (in Cadmium) as modeled by LECS package for Geant4 (triangles), in comparison to analytical computations (solid lines)

Lehner's notes for this figure are as follows.

The broadening, as shown in Figure 30, was calculated in the following manner. For a given Compton scatter angle and scattered gamma-ray energy, the projection of the momentum of the initial electron on the scattering vector is calculated as shown in Ribberfors and Berggren (1982), Eq. 17. This value is used to determine the atomic Compton profile, tabulated by Biggs, Mendelsohn, and Mann (1975). The double differential scattering cross section is then calculated as in Ribberfors and Berggren (1982), Eq. 21. The distribution for a given scatter angle was obtained by performing the above for all possible scattered gamma-ray energies. The Doppler broadening was calculated, as the full width for which 68% containment is achieved. This analysis was then repeated for angles between 0 and 180 degrees for a given initial gamma-ray energy.

It is clear that the analytical and Monte Carlo results match quite well. Note that analytical calculations use the atomic profiles in which an average profile is obtained by weighting each shell according to the number of electrons. LECS selects an electron shell and uses the tabulated profile for that specific shell. I expect the largest deviations between analytical calculations and LECS to occur at low energies and scatter angles, where shell effects become important.

Geant4 versions tested

All the testing discussed so far was done using Gean4 version 4.1.p01 and LECS version 1.01. We found Geant4 version 4.1p01 to be the most useful (stable) for the applications of interest to us. We realize however that other researches may be more interested in the latest versions of Geant4. Thus, a test of the most current Geant4 version was also conducted. Specifically, the combination of Geant4_5.2p01 and G4LECS_1.03 was compiled and tested in the same regime as earlier version Geant4_4.1p01/ G4LECS_1.01. The results of comparison of the two versions are presented in Figures 31 to 33.

Essentially, the results of both versions were found to be indistinguishable within the variation coming from the random number generator. The case where some differences between two versions can be observed is presented in Figure 31. Notice that all the differences are due to insufficient statistics and the random nature of Monte Carlo modeling.
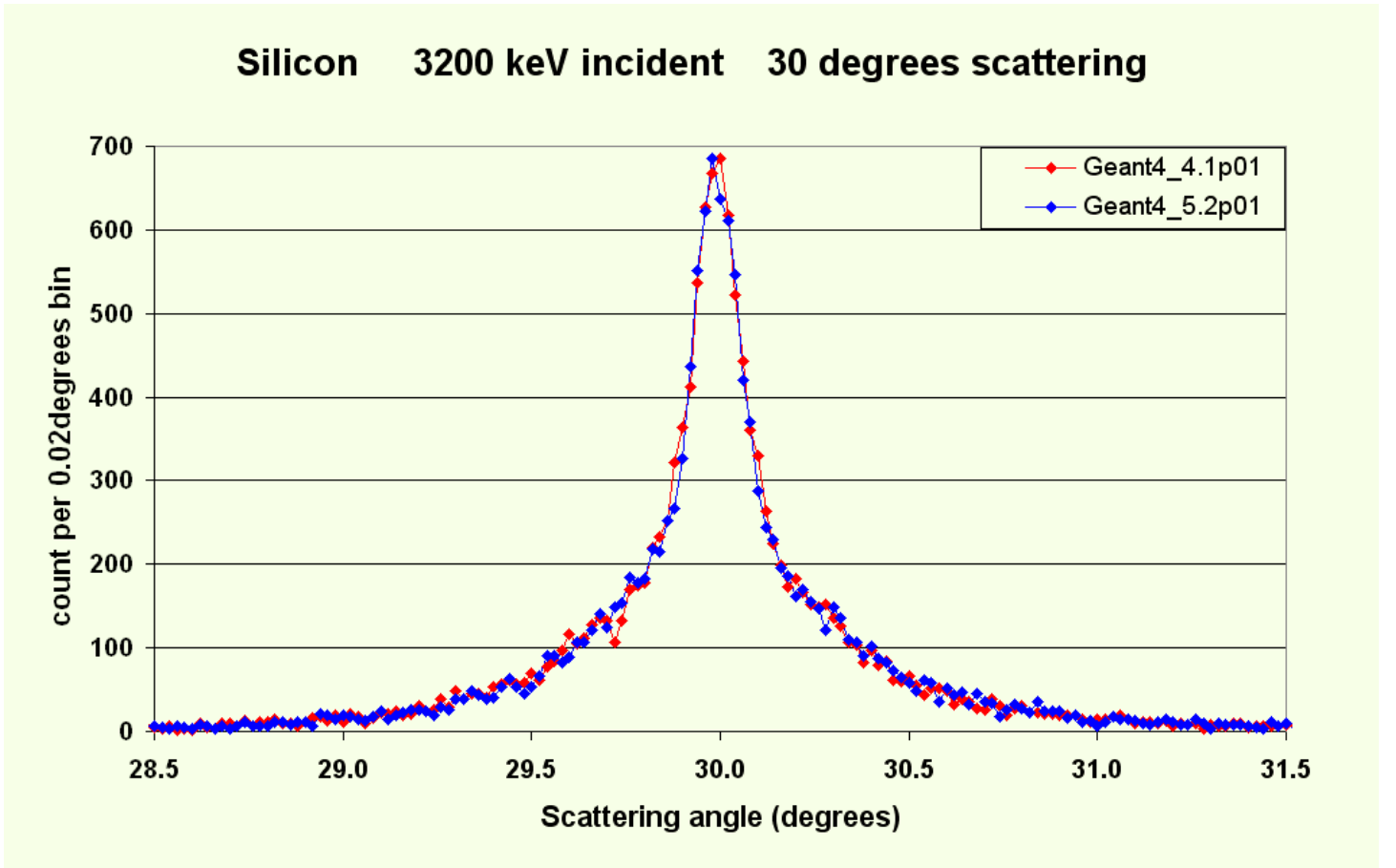

Figure 31. Comparison between versions Geant4_4.1p01/G4LECS_1.01 and Geant4_5.2p01/G4LECS_1.03. The distributions of the scattering angle of the gamma-ray in Silicon, for the incoming energy of 3200 keV. Only Compton interactions with the energy of the scattered gamma ray close to the energy corresponding to the scattering angle of 30 degrees in the absence of Doppler broadening were used. The "close" was defined as being within 0.015 keV of the exact value. Total number of incoming gamma-rays is 2 billion.

Similar to the case of Geant4_4.1p01/G4LECS_1.01 version, the width of the Doppler broadening for the case of Geant4_5.2p01/G4LECS_1.03 version was measured in two different regimes: as uncertainty in energy (for a fixed scattering angle) and as uncertainty angle (for a fixed scattering energy). Two materials were used as

targets, Silicon and Germanium. For each material, the same tests as those summarized in Figures 8 to 11 and 19 to 22 were run twice (with two different seeds used for the random number generator initialization). The results from the two runs using version Geant4_5.2p01/G4LECS_1.03 were compared to the single run made using version Geant4_4.1p01/G4LECS_1.01 (Figures 32 and 33).
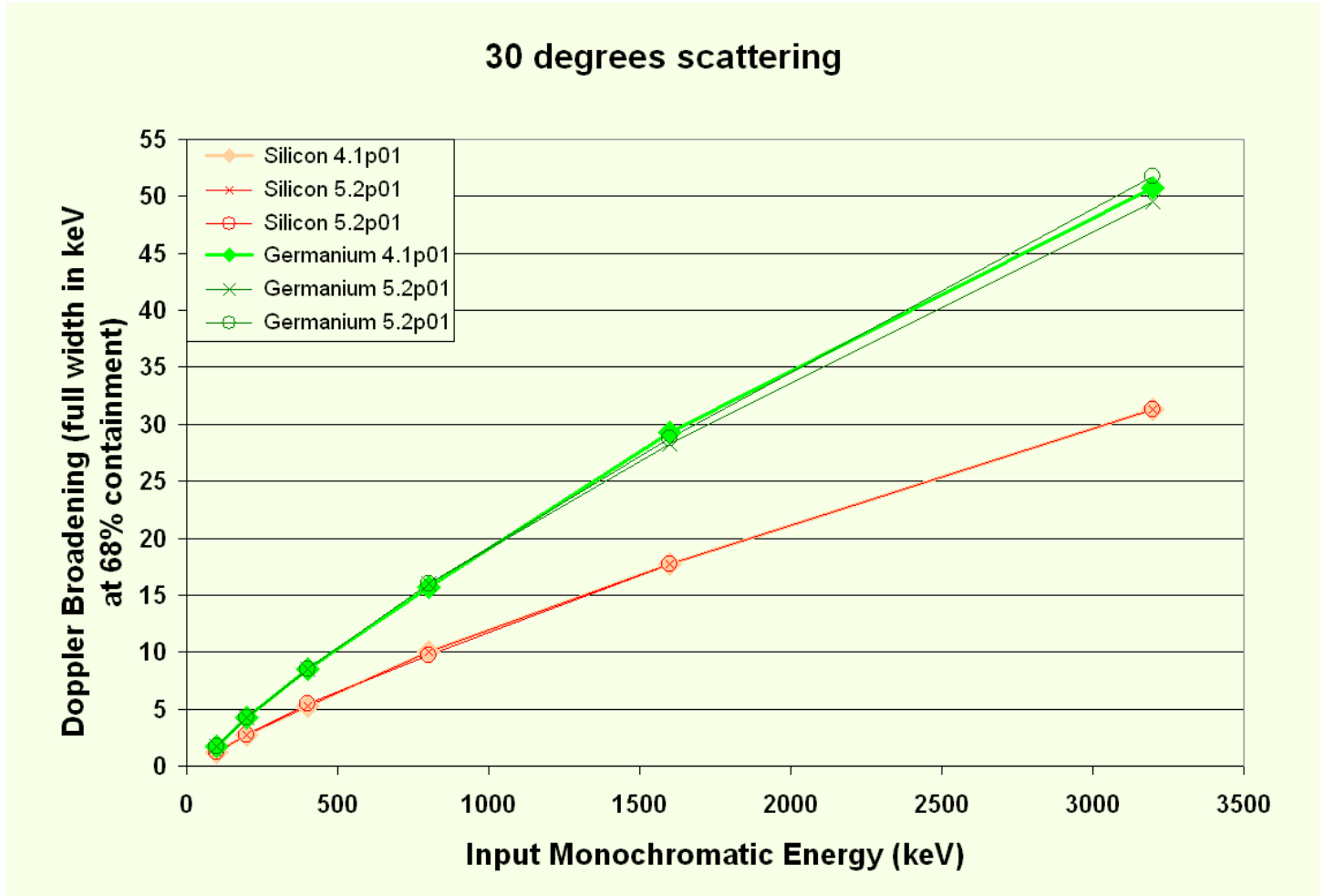

Figure 32. Comparison between versions Geant4_4.1p01/G4LECS_1.01 and Geant4_5.2p01/G4LECS_1.03. Doppler broadening as a function of the energy of the incoming gamma-ray. Broadening was measured in keV, as the full width at 68% containment for the distributions of the energy of the scattered gamma-ray, for Silicon and Germanium. Only Compton interactions with the scattering angles from 29.99 to 30.01 degrees were used. There were two independent runs made using version Geant4_5.2p01/G4LECS_1.03 (with different seed used for the random number generator). The same data as those shown in Figure 8 are used for the Geant4_4.1p01/G4LECS_1.01 version.
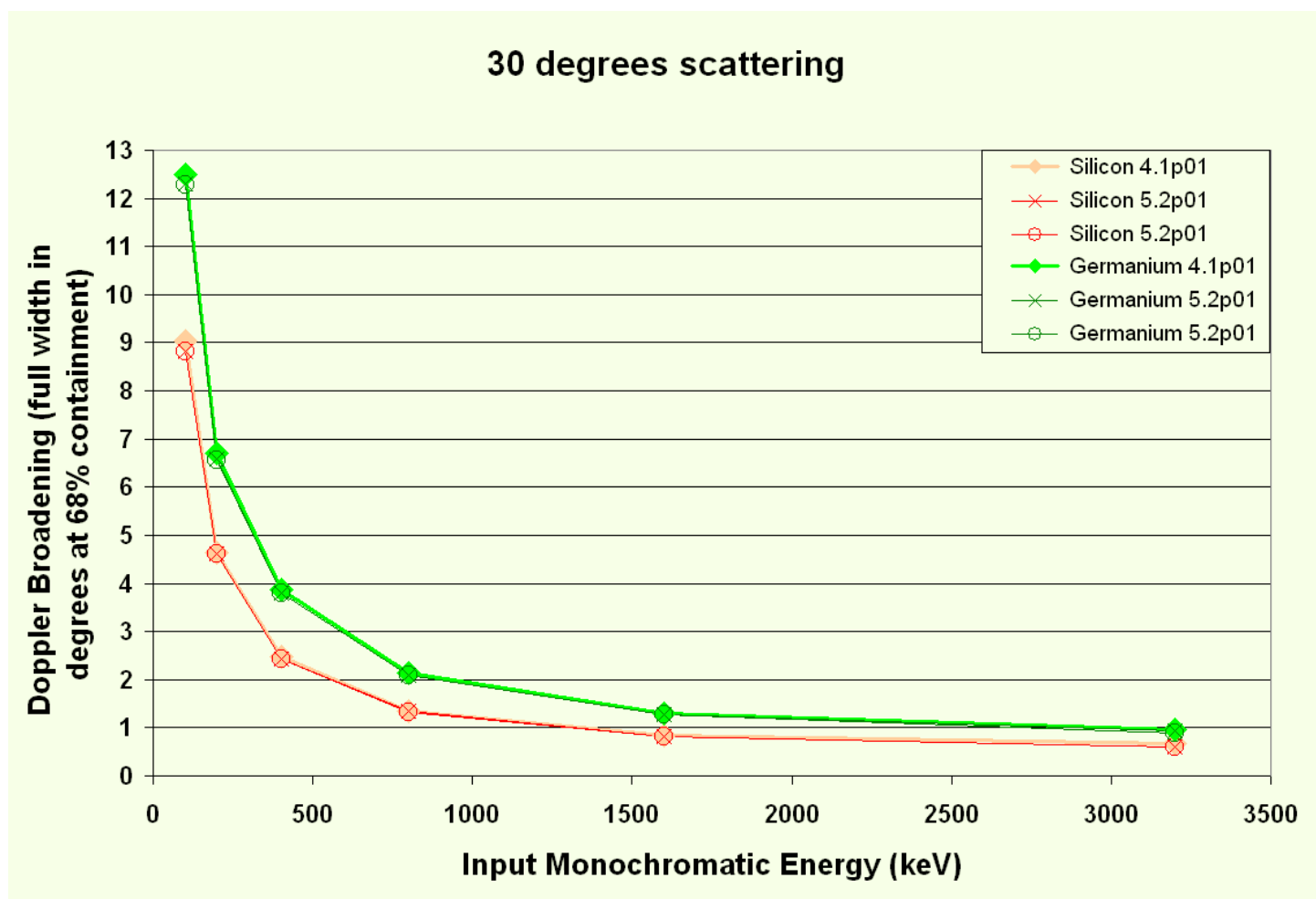
Figure 33. Comparison between versions Geant4_4.1p01/G4LECS_1.01 and Geant4_5.2p01/G4LECS_1.03. Doppler broadening as a function of the energy of the incoming gamma-ray. Broadening was measured in degrees, as the full width at 68% containment for the distributions of the scattering angle of the scattered gamma-ray, for several materials. Only Compton interactions with the energy of the scattered gamma ray close to the energy corresponding to the scattering angle of 30 degrees in the absence of Doppler broadening were used. The "close" was defined as being within 0.015 keV of the exact value. There were two independent runs made using version Geant4_5.2p01/G4LECS_1.03 (with different seed used for the random number generator). The same data as those shown in Figure 8 are used for the Geant4_4.1p01/G4LECS_1.01 version.

Based on the presented results a conclusion can be made that both versions of the Doppler broadening, Geant4_4.1p01/G4LECS_1.01 and Geant4_5.2p01/G4LECS_1.03, work equally well and produce identical (within the random number generator jitter) results.

Conclusions

Our testing has shown that LECS is a valuable addition to the Geant4 package. It represents physics that is needed for modeling Compton interactions in the energy range below 10 MeV. It is especially needed for the modeling of Compton gamma ray detectors. The output of the LECS package agrees well with independent analytical estimates.

LECS package is extremely easy to install. The package is highly reliable C++ wise. It worked without a single glitch throughout hundreds of billions of events in our testing.

We recommend this package to be included into standard (downloadable from the Geant4 Home page http://geant4.web.cern.ch/geant4/) version of Geant4, ASAP.

References

C. Michael Lederer and Virginia S. Shirley, Table of Isotopes (seventh edition), National Standard Reference Data System, Department of Energy, 1978.

Ribberfors and Berggren, Incoherent x-ray-scattering functions and cross sections by means of a pocket calculator, Phys. Rev. A. Vol 26, No. 6, 1982, pp. 3325-3333.

Biggs, Mendelsohn, and Mann, Hartree-Fock Compton profiles for the elements, Atomic and Nuclear Data Tables, Vol. 16, 1975, pp. 201-309.